Retinal degeneration in and *in vivo* electroretinography measurements of Smoky Joe Chickens

by

Thanh Tan Tran

A thesis

presented to the University of Waterloo

in fulfillment of the

thesis requirement for the degree of

Master of Science

in

Vision Science and Biology

Waterloo, Ontario, Canada, 2012

AUTHOR'S DECLARATION

I hereby declare that I am the sole author of this thesis. This is a true copy of the thesis; including any required final revisions, as accepted by my examiners. I understand that my thesis may be made electronically available to the public.

ABSTRACT

Inherited retinal degenerative diseases can affect various components of the retina leading to blindness. Five different mutant strains of chicken have been studied extensively as potential models for inherited retinal degeneration. The Smoky Joe (SJ) chicken is a sixth genetically blind strain of White Leghorns that shows various degrees of blindness at hatch and by 8 weeks post-hatch, have complete blindness for those that are homozygous. The objective of this study was to characterize the retinal degeneration in these birds by histology, both during embryonic and post-hatch development, and to the retinal function using electroretinograms (ERG). For both embryonic and post-hatch development, a significantly lower number of cells were found in the retina of blind birds compared to sighted (both $p<0.0001$). The significant contributor to cell number decrease was the loss of amacrine cells located in the inner nuclear layer. Photoreceptors were also found to potentially decrease in number, but at a later stage. ERG recordings revealed decreases in amplitudes of b-waves and oscillatory potentials in blind birds, but not in sighted. Both histology and ERG findings support the idea that the inner retinal cells are affected. The results indicate that degeneration in the Smoky Joe retina occurs mostly within the inner nuclear layer affecting amacrine cells. This hampers the functional capacity of the retina, causing blindness.

ACKNOWLEDGEMENTS

I would like to thank, first and foremost, my supervisor Dr. Vivian Choh for giving me the opportunity to do research. I want to thank her for her time, effort and knowledge in helping and guiding me through this Master's. In addition, I want to thank her for taking a chance on me and entrusting me with this project. I also want to thank my committee members Dr. Jacob Sivak and Dr. Mungo Marsden for their guidance throughout the project that helped me through my goals. Dr. Bernard Duncker for giving me my initial research experience necessary to even start a Master's and Dr. Gregoy Bedecarrats for collaborating with us and providing the Smoky Joe chickens.

I want to thank my lab-mates Stacey Chong and Gah-Jone Won for helping me with anything that I needed in the lab. As well for keeping me company during my second year of Master's, because the lab was real quiet during my first. I would like to thank all the graduate students and GIVS for their inclusion and making my time here remarkably memorable from the lunch outings, intramurals to ARVO trips. Outside the lab, I want to thank Nancy Gibson for looking after my chicks week to week. To Nancy MacNeil for a great fun time TAing, I learned a lot.

I also owe a bunch to my family for their constant support in my educational endeavors. I know it's not easy letting me go off to school away from home for so long. Lastly, I want to thank Cecilia, my other half, who's stood beside me throughout my years here in Waterloo, especially those when she wasn't here. I know this Master's project has been tough on her at times when we're not able to be together. Massive thanks to her for understanding and caring, and I hope that we'll keep standing beside each other for many years to come.

TABLE OF CONTENTS

LIST OF FIGURES

LIST OF ABBREVIATIONS

AChE ..... acetylcholinesterase
AMD ..... age-related macular degeneration
Beg ..... blindness enlarged globe
bHLH ..... basic helix-loop-helix
ChAT ..... choline acetyltransferase
D1 ..... day 1 post-hatch
DAM ..... delayed amelanotic
DAPI ..... 4', 6-diamidino-2-phenylindole
E1 to E22 ..... embryonic day 1 to 22
ERG ..... electroretinogram
FABP ..... retinal fatty acid binding protein
FFT ..... Fast Fourier Transform
FGF-1, FGF-2 ..... fibroblast growth factor
FITC ..... Fluorescein Isothiocynate
GABA ..... Gamma-aminobutyric acid
GCL ..... ganglion cell layer
GFAP ..... glial acidic filament protein
GS ..... glutamine synthetase
ISCEV ..... International Society for Clinical Electrophysiology of Vision
INBL ..... inner neuroblastic layer
INL ..... inner nuclear layer
IPM ..... interphotoreceptor matrix
LCA ..... Leber congenital amaurosis
mfERG ..... multi-focal electroretinography
Mitf ..... microphthalmia-associated factor
ONBL ..... outer neuroblastic layer
ONL ..... outer nuclear layer
OP ..... oscillatory potential
OPL ..... outer plexiform layer
PBS ..... phosphate buffered saline
pERG ..... pattern electroretinography
rd ..... retinal degeneration
rdd ..... retinal dysplasia and degeneration
r-FABP ..... retinal fatty acid binding protein
rge ..... retinopathy globe enlarged
RP ..... retinitis pigmentosa
RPE ..... retinal pigment epithelium
SJ ..... Smokey Joe
TRITC ..... Tetramethyl Rhodamine Isothiocyanate
VB ..... vecuronium bromide
VnRK ..... visinin-negative rhodopsin kinase
W1 to W9 ..... week 1 to week 9
WGA ..... wheat germ agglutinin

I. LITERATURE REVIEW

1.1. Development and anatomy of the vertebrate eye

The initiation of eye development begins with the evagination of the brain to form the optic vesicles. Contact of the optic vesicle with the overlying ectoderm induces a thickening of the latter layer leading to the formation of the lens placode (O'Rahilly and Meyer, 1959). The lens placode then invaginates on itself and separates from the surrounding tissue to ultimately form the lens (Kuszak et al., 1980). Optic vesicle formation occurs simultaneously with the lens. When the vesicle extends and contacts the surface ectoderm, the vesicles invaginate to form the optic cup. Continued development of the optic cup allows for the formation of the inner neural layer and the outer pigment epithelial layer. The mesenchymal cells work their way in between the surface ectoderm and the lens and give rise to the stroma and endothelium of the cornea. Development of the sclera starts following condensation of paraxial mesenchyme surrounding the optic cup and develops in two stages, the anterior and posterior sclera.

The stroma of the iris develops from the mesenchyme while the anterior tip of the optic cup scaffolds under the stroma to form the layered pigment epithelium of the iris (Snell and Lemp, 1989; Warwick and Williams, 1973). The pupillary membrane is formed by the mesenchymal tissue around the margin of the optic cup. The periphery portion of the pupillary membrane gets vascularized while the central part is absorbed and forms the pupil. Finally the choroid, a darkly pigmented and highly vascular connective tissue layer, consists of two parts mostly developping from the mesenchymal membrane. Vasculature development begins with the choriocapillaris and ultimately forms choroidal arterioles and venules (Sellheyer, 1990).

1.1.1. Development of the retina: RPE

Each of the two layers that make up the optic cup, the inner and outer layer, forms the neural

retina and the retinal pigment epithelium (RPE), respectively. At this relatively early stage in development, the progenitor cells of the optic vesicles remain multi-potent having the ability to become cells either of the neural retina or of RPE (Hyer et al., 1998). For RPE differentiation, RPE cells are subject to the control of the protein microphthalmia-associated transcription factor (Mitf), produced by the mesenchyme. These Mitf proteins initially accumulate in the RPE precursor cells. Mitf protein inhibits the synthesis of the retinal transcription factor Pax-6 and induces the pigmentation of RPE cells (Mochii et al., 2011). Other genes that may regulate RPE development include the Homeobox-containing gene *Otx2* that initiates distinct expression patterns in the dorsal portion of the optic vesicles when in contact with the surface ectoderm. It is then localized to cells of the outer layer of the optic cup following a central to peripheral pattern (Bovolenta et al., 1997). It is sugguested that Otx2 is necessary for RPE determination of the outer layer.

1.1.2. Development of the retina: Neural retina

Previous studies have focused on the acidic and basic fibroblast growth factors (FGF-1, FGF-2) for retinal development due to the discovery of the RPE's ability to regenerate the neural retina if it was surgically removed, as seen in chick embryos (Coulombre and Coulombre, 1965). Park and Hollenberg (1989) also found that after removing the neural retina from chick embryos, the pigmented epithelium was stimulated specifically by FGF-2 to regenerate the neural retina (Park and Hollenberg, 1989). These fibroblast growth factors are are seen as necessary for the differentiation and development of the neural retina. Furthermore, cell culture experiments have shown that FGF-2 neutralizing antibodies inhibit the development of the neural retina and not of the RPE (Pittack et al., 1997). The FGFs derived from the surface ectoderm therefore drives the differentiation of neural retina development from that of the RPE

(Hyer et al., 1998).

As the developing cells proliferate and differentiate into various retinal cell types, their migration and the growth of cellular projections form the typical neuron cell structures. Once the cell projections are formed, development is complete at around embryonic day 16 (E16) in chickens (Mey and Thanos, 2000). Migratory movements and/or arrested movements of the neuroblastic cell soma are required to form the layers of the retina. Initially, a transient fiber layer divides the retinal epithelium into two layers consisting of the inner and outer neuroblastic layers (Willbold and Layer, 1992). At this early stage, the inner neuroblastic layer contains newly developed neurons, mostly amacrine and ganglion cells, while the outer neuroblastic layer contained mitotic progenitor cells. Once the migratory process is completed, three nuclear layers can be characterized by the various cell types seen in a mature retina (Figure 1), the ganglion cell layer (GCL) containing displaced amacrine cells and ganglion cells, the inner nuclear layer (INL), containing amacrine cells, displaced ganglion cells, bipolar cells, horizontal cells, and Müller cells, and the outer nuclear layer (ONL), containing the photoreceptors (rod and cone cells).

1.2. Development of neural retinal cell types in chickens

1.2.1. Retinal ganglion cells

Of the retinal cell types, the ganglion cells are of significant interest to many researchers due to their important role in vision sensory transduction, as well as in nerve regenerative studies. Different ganglion cells in chick can be identified based on their location, size and form of their cell body, and shapes of their dendrites (Thanos et al., 1992). At the molecular level, neurotransmitters that seem to be present in the majority of the retinal ganglion cells are glutamate and/or aspartate (Beaudet et al., 1981). Also present in avian ganglion cells are

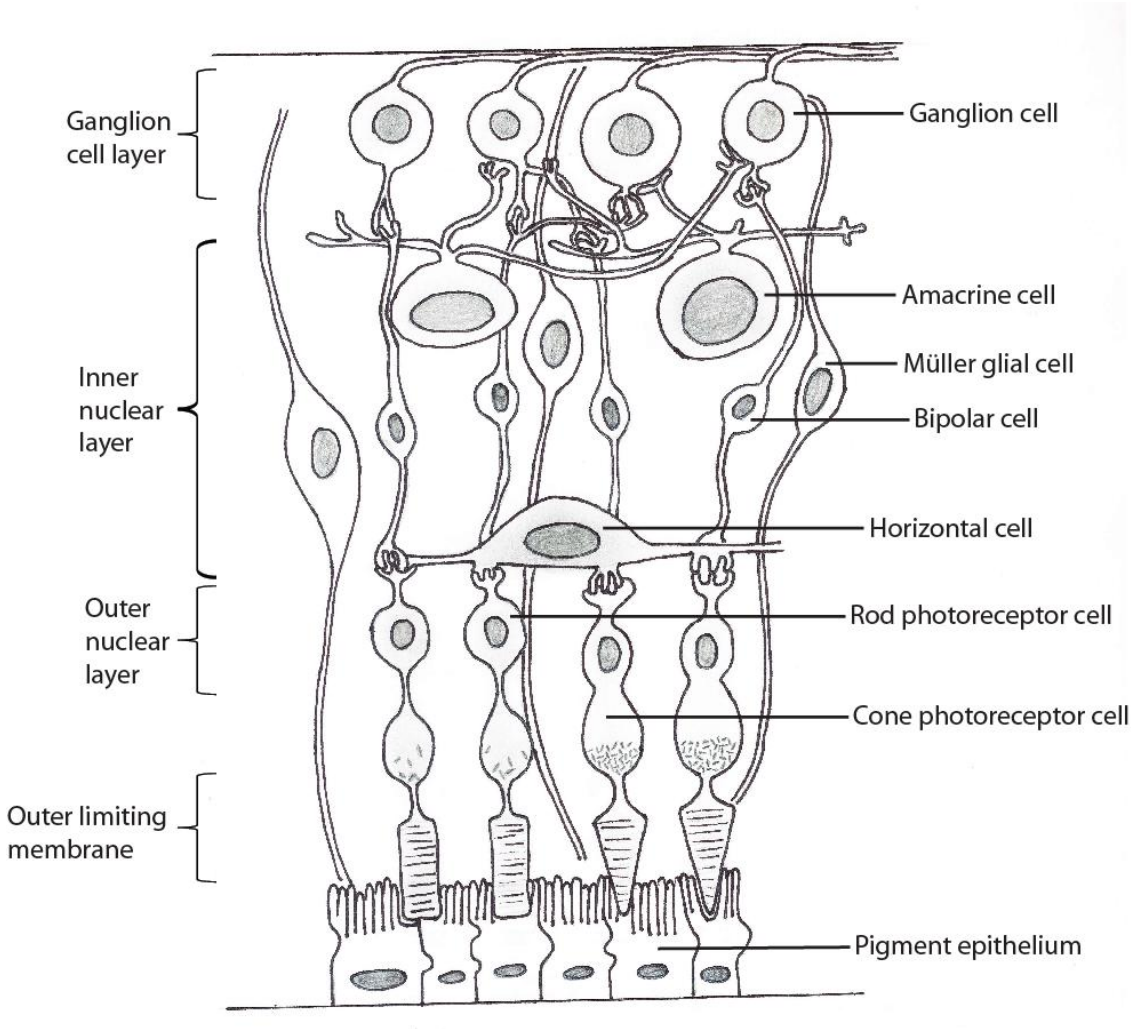

Figure 1. Diagram of mature retina with all neuronal cell types and supportive Müller glial cell within the various nuclear layers. ONL, outer nuclear layer; INL, inner nuclear layer; GCL, ganglion cell layer. (Drawing by Cecilia Pham).

catecholamines and peptides (Yamagata and Sanes, 1995). Displaced ganglion cells, with their soma located in the INL, also use catecholamines (Britto et al., 1988).

As the first cells begin to differentiate, ganglion cell neuroblasts detach themselves from the ventricular surface of the optic vesicles and posteriorly migrate towards the inner limiting membrane, forming the GCL (Prada et al., 1981; Watanabe et al., 1991). Before migration, the ganglion cells are able to extend their processes, or endfeet, to contact both sides

of the retina, which then allows for their migration. After detachment of the processes, the vitreal endfoot will transform and become the axon (Watanabe et al., 1991; Nishimura, 1980). In chicks, the ganglion cells complete development at around E16, before hatch. Note that programmed cell death occurs by apoptosis of the ganglions between E11-E16 (Hughes and McLoon, 1979) to eliminate any unnecessary connections that have been made. Retinal ganglion cells that project to the central visual targets of the tectum have the ability to withstand and survive the apoptosis progression (Vanselow et al., 1990). This ability to preferentially kill off unrequired ganglion cells and their differential expression creates a gradient of ganglion cells across the retina (Straznicky and Chehade, 1987) with the highest density of ganglions, as well as photoreceptors, located within a central region called the fovea or area centralis (Ehrlich, 1981).

1.2.2. Photoreceptors: rods and cones

Photoreceptors have been noted to exit the cell cycle early in embryonic development and begin differentiation; however they require longer periods of time to complete maturation. In chickens, photoreceptor neuroblasts begin to extend their inner segments towards the subretinal space and RPE at E9, at which point the initiation of their morphogenesis occurs (Olson, 1979). Photoreceptor inner segments contain numerous microvilli that help the cell-to-cell interactions with each other and Müller cells. Subsequently, the outer segments will protrude from the inner at around E21. Normal electrical responses to light stimulus by photoreceptors develop between E17 and postnatal day 3 (Hanawa et al., 1976).

The chicken retina is cone dominant, composed of four different types of cone cells and one type of rod cell, all identified by the type of light sensitive pigments they contain. The rod cells are characterized by rhodopsin whereas cones are divided into red-, green-, blue- and

ultraviolet/violet-cone opsins (Araki et al., 1990; Okano et al., 1992). Red and green opsin cones are expressed first during development, followed by rhodopsin rods, blue and violet opsin cones (Bruhn and Cepko, 1996), but all these appear quite late in development.

There are also various calcium receptors that begin to arise late in development. Calbindin, visinin, guanylate cyclase-activating protein 1 + 2 are all expressed in photoreceptors during the final week of embryonic development. Visinin is unique as it is also present beginning early in development at E7 in areas where photoreceptors are mostly cone cells with lower concentrations of rod cells (Bruhn and Cepko, 1996). Lastly, the neurotransmitters that photoreceptors use for signal transduction toward bipolar and amacrine cells are glutamate and aspartate (Biziere and Coyle, 1979).

One of the key differences between photoreceptors in mammals and birds is the presence of brightly colored filters in birds called oil droplets. Although the adaptive advantage remains unclear there are studies that speculate the ability of oil droplets to reduce chromatic aberration, that is the inability to focus colours on a convergent point, and to increase the number of colours that can be discriminated (Vorobyev, 2003).

1.2.3. Müller cells

Early on in development, Müller glial cells cannot be morphologically identified from other undifferentiated neuroblast cells. A later distinguishing marker for Müller cells, much like other astrocytes within the central nervous system, is the glial acidic filament protein (GFAP) (Ikeda et al., 1980). When the Müller glial cells form synaptic connections within the outer plexiform layer (OPL), the Müller cell processes extend towards the basal surface of the retina. Müller cell processes enclose bipolar cells while their basal protrusions contact the ganglion cells axons. The enzyme glutamine synthetase is important for recycling the synaptic

glutamate within the retina in which Müller cells uptake the glutamate to allow glutamate conversion into glutamine (Winkler et al., 1999). Thus Müller cells are the major contributing cell glutamine synthetase synthesis within the OPL (Prada et al., 1998).

1.2.4. Amacrine, horizontal and bipolar cells

Amacrine and horizontal can be morphologically identified by E14 in chickens. Amacrines use a range of transmitters for their synaptic transduction and they are classified by which transmitter they use. Similar to photoreceptors, amacrines exit the cell cycle early with a one-week delay in the morphology. For example, development of dopaminergic amacrine cell soma occurs between E3-E7 when it migrates into the INL, but do not differentiate morphologically, i.e. the development of their primary dendrites, until E14. Choline acetyltransferase (ChAT) and acetylcholinesterase (AChE), related enzymes that synthesize and metabolize acetylcholine, are expressed in cholinergic amacrines before any synaptic connections are completed (Spira et al., 1987).

Gamma-aminobutyric acid (GABA) is an inhibitory transmitter that is found to be produced in dopaminergic amacrine and horizontal cells (Wulle and Wagner, 1990). Horizontal neuroblasts cells begin to migrate at E13-E15 and develop GABA-immunoreactive projections that extend towards the OPL. One of these projections will give rise to the horizontal cell axon at E14. These dendrites then form synaptic contacts with cone photoreceptors.

Bipolar cells are one of the last cell types to withdraw from the cell cycle. At the same time, they are the last to differentiate from their neuroblastic state into mature bipolar cells and to localise to the INL. Their connections to photoreceptors do not complete until after E17 (Quesada et al., 1986).

1.3. Degenerative diseases of the retina

1.3.1. Retinitis pigmentosa (RP)

An inherited retinal disease that affects approximately 1 in 4000 in the general population, retinitis pigmentosa (RP) is characterized by progressive photoreceptor cell degeneration (Hamel, 2001). The RP group of diseases can differ in the age of onset, the severity and the genetic inheritance. The retinal degeneration that occurs because of RP initially starts in the mid-peripheral area of the retina and slowly migrates towards the macula and fovea. Through microscopic examinations, the retinas of RP patients showed an absence of rod photoreceptor cells and the presence of abnormal pigment epithelium cells with few cone photoreceptors (Kolb and Gouras, 1974; Mizuno and Nishida, 1967; Szamier et al., 1979). Therefore, the most common form of RP is a rod-cone dystrophy in which night blindness is the first symptom to materialize, followed by progressive loss of the visual field in the periphery.

Since rods in RP drive photoreceptor degeneration, electrophysiological recordings (ERGs) have shown that the rod responses from ERG are affected more severely than the cones. But as the disease progresses to an advanced stage, both rod and cone ERG responses are abolished.

1.3.2. Leber congenital amaurosis (LCA)

Leber congenital amaurosis (LCA) was initially described as a congenital form of RP that is transmitted as an autosomal recessive disorder (Koenekoop, 2004). In children, LCA has been documented to be the most severe and common reason of congenital blindness. The genes associated with LCA are quite numerous, affecting various aspects of the retina, including retinal development, phototransduction, RPE phagocytsosis etc. (Den Hollander et al., 2008). Depending on the gene affected, various cell types have been shown to be degenerative in

different cases. In addition, the electroretinograms of LCA individuals show extinct or severely abnormal responses of the entire waveform (Franceschetti and Dieterle, 1954).

1.3.3. Age-related macular degeneration (AMD)

Age-related macular degeneration (AMD) is a condition affecting the RPE, the supportive basement membrane of the RPE and the overlying photoreceptors. The leading cause of blindness among the population who are 65 years and older, AMD is generally characterized by small deposits of extracellular material, called drusens, under the RPE (Bird, 1992). Though not pathogenic, if these drusens continually grow and enlarge, a loss of RPE cells at the deposit region can occur, leading to eventual photoreceptor degeneration. As the disease progresses with age, further physiological processes can contribute to the AMD such as inflammation, oxidative damage and RPE senescence (Hageman et al., 2001).

As with many disease studies, animal models provide valuable insights into etiologies of RP, LCA and AMD. Although many studies utilize mice, rats, cats and dogs, inherited degenerative ocular anomalies in chicken may provide different and additional models for these retinal diseases.

1.4. Electroretinography (ERG)

The induction of electrical activity in the eye due to light stimuli encompasses the basic principles of an electroretinogram (ERG), where changes of electrical activity, specifically in the retina, can be monitored and measured. ERGs are now used as a diagnostic tool that measures the electrical activity of the retina and allows assessment of retinal function.

The full-field (ganzfield) light-induced ERG is the conventional simple form of ERG that measures a diffuse electrical response from cells of the retina following a stimulant flash of light. The ERG response can be separated into three major waves ERG: a-, b- and c-waves

(Figure 2). Each wave is a representation of activity from different functional cells of the retina. When the waves were first described, it was suggested that the light stimulus causes a series of reactions inducing a change in electrical activity leading to the formation of these waves (Einthoven and Jolly, 1908).

In addition to wave separation of the ERG response, the ERG has also been divided into three different components: P-I, P-II and P-III (Figure 2). These components are not discrete reactions, but rather, last over the duration of the light stimulus. From the Granit study (1933), it is understood that the negative a-wave is the equivalent to the leading edge of the P-III component. The b-wave is a result of the addition of the P-II and PIII components together while the c-wave is the addition of the P-I and P-III. These components and the resulting waveforms remain the principle behind the understanding of ERGs.

The next step in the understanding of ERGs is to correlate the wave components to cellular components of the retina. The P-III component can be divided into two parts: a fast P

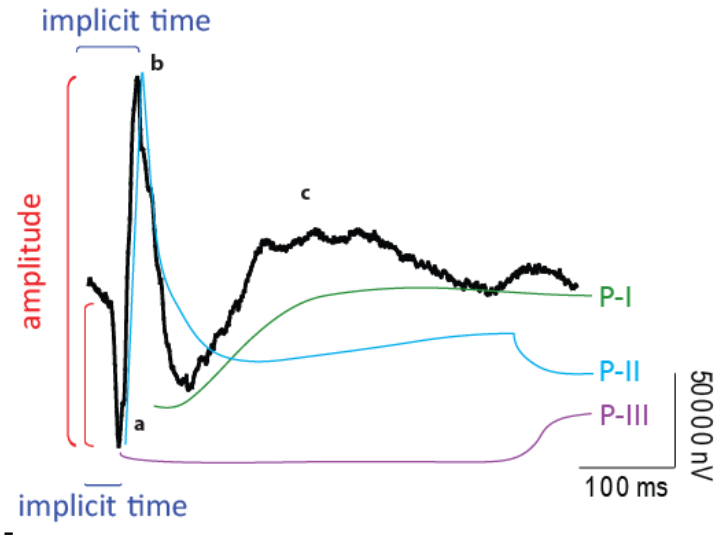

Figure 2. Typical chicken ERG response from data set (black) to a 4 ms long light stimulus at a flash intensity 3.16 cd.m/s2 showing a-, b- and c-waves and additional components P-I (green), P-II (light blue) and P-III (purple). Amplitude (red) and implicit time (dark blue) are parameters to be analyzed for a- and b-waves.

III and a slow P-III (Murakami and Kaneko, 1966; Sillman et al., 1969). Studies using intra-retinal microelectrodes in rat revealed that the fast P-III is a result of photoreceptor activity (Brown and Wiesel, 1961; Tomita, 1950). To further confirm that photoreceptors are the origins of the fast P-III component and ultimately part of the a-wave, chemical inhibitors of photoreceptor neurotransmitters were used to block photoreceptor synapses. These drugs isolated the response of the photoreceptors, where only the a-wave was detected in the ERG and no evidence of a b-wave existed, providing evidence of the fast P-III nature. The slow P-III component normally cannot be detected in a regular ERG because of the overriding effects of the larger amplitude from the P-I wave. Witkovsky and colleagues (1975) however isolated the slow P-III component and found that glial Müller cells are the cells to generate this component (Witkovsky et al., 1975).

Different methods of blocking and affecting the post-synaptic transmission of photoreceptors have been shown to abolish the b-wave component of a normal ERG (Brown and Watanabe, 1962; Pepperberg and Masland, 1978; Sillman et al., 1969). Which type of cells makes up the origins of the b-wave has been extensively studied, including those for Müller cells and specific bipolar cells. To test the "Müller-cell hypothesis", experiments using barium ions, which block membrane potential in Müller cells, revealed no decrease in the treated ERG b-wave but rather that the b-wave was augmented (Lei and Perlman, 1999). Therefore, these results support bipolar cells as the major contributors of the b-wave. The b-wave can also be influenced by third order neurons (amacrine and ganglion cells) in terms of its amplitude and kinetics (Dong and Hare, 2000).

The final, c-wave component of the ERG is interpreted as a response from the RPE. Removal of the RPE from the retina of skate eyecups showed ERG recordings with a- and b-

waves only (Pepperberg et al., 1978). The c-wave component was not detected when the RPE was not present. The mechanism by which the c-wave occurs is based on the constant potential differences between the positive-retina relative to the choroid. When there is light induction, the photoreceptor causes a reduction of the extracellular potassium ion concentration, which leads to a trans-epithelial potential difference in the RPE cells, making the retina more positive compared to the choroid. This finding shows that the c-wave represents the functional interaction between both RPE and photoreceptor cells.

1.4.1. Oscillatory potentials (OPs)

Additional components of the ERG waveform that are important clinically and experimentally are the oscillatory potentials (OPs). OPs are low amplitude wavelets found primarily on the rising phase of the b-wave. In order to isolate the OPs and to better visualize them, it is recommended by the International Society for Clinical Electrophysiology of Vision (ISCEV) that a band-pass filter be used on the ERG to eliminate the slower and larger amplitudes of the a- and b-waves (Asi and Perlman, 1992). Following the proper digital filter, the isolated OPs can have a Fast Fourier Transform (FFT) applied in order to obtain a power spectrum. The FFT allows for the assessment of the amplitude and frequencies of the OPs. In terms of the cellular origin of the OPs, there is still much debate. There have been pharmacological studies where injections of glycine cause morphological changes in many amacrine cells in the rabbit retina and results in the disappearance of the OPs (Korol et al., 1975), which suggest a role for amacrine cells in OPs. It was also found that in the mudpuppy retina, the first OP originated at the retinal depth of the amacrine cells (Wachtmeister and Dowling, 1978). Other studies have suggested that generation of OPs may also be from ganglion cells (Ogden, 1973; Steinberg, 1966) and bipolar cells (Heynen et al., 1985).

1.4.2. Multi-focal electroretinography (mfERG)

Anomalies in the full-field ERG response usually only arise when there are large areas of the retina that are functionally impaired. Focal ERGs (fERGs) were developed to allow for the targeting of specific areas in the retina that might be diseased and that cannot be detected with a full-field ERG. The fERGs are becoming more useful in determining the functional activity of the macula.

Further advances in technology have allowed for the development of what is called multi-focal ERGs (mfERGs). mfERGs measure multiple retinal responses at different locations simultaneously, meaning that it allows for mapping of retinal function in the central 40-50° of the retina (Lai et al., 2007). The traditional stimulus for mfERG consists of a large number of arrays displayed on a video monitor. The output is then composed of multiple mini waveforms in a topographic arrangement. An mfERG simulating the parameters of the full-field ERG was measured, tested and compared to the normal ERG. The negative wave of the mfERG represent the same components as the a-wave in the full-field ERG; in addition the cell types of the positive wave of the mfERG are similar to that of the positive b-wave of the full-field ERG (Hood et al., 1997). The power of the mfERG is in the fact that each of its mini outputs reflects all the components of the retina.

1.4.3. Pattern electroretinography (pERG)

Simply, a pattern electroretinogram (pERG) is the retinal response one gets when a structured stimulus is used, for example a reversing checkerboard pattern. This stimulus allows for assessment of small electrical potentials that originate at the level of the inner retina, in association with macular function. Studies of the positive wave at 50 ms (P50) and the negative wave at 95 ms (N95) of the pERG have not quite deduced which particular cell types

are triggering these wave forms. Studies of optic nerve section in cats (Mafei and Fiorentini, 1981) and monkeys (Maffei et al., 1985) produced pERG extinction following degeneration of retinal ganglions cells, indicating ganglion cell generation of pERG, presumably in the P50. Studies that looked into the spatial tuning properties of the pERG, in which the P50 component did not show low spatial frequency suggested that partial pERG originates from non-ganglion cells (Kirkham and Coupland, 1983; Trick and Wintermeyer, 1982). It is now postulated that the N95 arises from ganglion cells, and that P50 does have origins in the ganglion cell but there are partial effects from more distal parts of the retina.

1.4.4. Flicker ERG (fERG) and Scotopic Threshold Response (STR)

There are many ways in which ERG recordings can be manipulated and changed to serve specific needs. ERGs using different rates of stimulus, also referred to as flicker ERG (fERG), enables the separation of rod and cone cell contributions to the ERG response. Under optimal conditions rod cells are unable to detect flickering light up to 20 Hz, whereas cones have a much easier time with higher frequency (Goto et al., 1998). Normal flicker stimulus is around 30 Hz to assess cone function.

The scotopic threshold response (STR) is a postreceptoral potential ERG response that originates from the proximal retina, in which amacrine and ganglion cells are found. The STR is recorded following dark-adaption under scotopic conditions with very weak flash stimuli. A negative response which has opposite polarity is induced, and the response is more sensitive than that of the b-wave (Sieving et al., 1986).

1.5. Mutant chick strains of inherited retinal degeneration diseases

The five mutant strain of chickens that have been documented include the retinopathy globe enlarged (*rge*), the blindness enlarged globe (*beg*), the retinal dysplasia and degeneration strain

(*rdd*), the retinal degeneration (*rd*) and the delayed amelanotic (DAM) strains. Understanding their clinical, histological and electrophysiological characteristics is important towards correlating these models to human diseases.

1.5.1. Retinopathy globe enlarged (rge)

The *rge* chickens have an autosomal recessive mutation that affects the cone β-transducin gene. This mutation leads to an enlargement of the globe and blindness (Curtis et al., 1987). Within the first few weeks, the cornea becomes thicker and the chicks display symptoms of hyperopia (Montiani-Ferreira et al., 2003). In addition, the anterior chamber becomes shallower. ERG measurements of the *rge* chicks show smaller a-wave amplitudes, a lack of OPs and c-wave, and an increase in b-wave amplitude (Montiani-Ferreira et al., 2007). There is also a general progressive decrease in overall ERG amplitudes, which coincides with a thinning of the photoreceptor layer. This evidence suggests that the mutation may have effects on photoreceptors and inner retinal cells.

1.5.2. Blindness enlarged globe (beg)

Observed as an autosomal recessive mutant, the *beg* chicks are blind at hatch. The overall size of the eyes from affected birds is much larger compared to normal chick eyes. The mutation often causes a large number of holes in the retina of the embryos of this mutant strain. These holes continually grow in diameter and eventually span the region between the RPE and the external limiting membrane. In adult chicks, degeneration of the photoreceptors is in the outer nuclear layer, while the RPE contains irregular clumps (Pollock et al., 1982).

1.5.3. Retinal dysplasia and degeneration (rdd)

Found to be an inherited recessive mutation in a single gene, one of the retinopathic characteristics of the *rdd* birds includes a progressive degree of blindness. At hatch, the

affected chicks are sighted for only up until 5-6 weeks, when they begin to show signs of visual impairment. From this point on, the chicks slowly start to lose their vision until they reach sexual maturity when they become completely blind (Randall et al., 1983). Histologically, small white holes within the retinal pigment epithelium (RPE) are seen at embryonic day 8 and these progressively become larger until hatch. After hatch, the RPE holes disappear and the layer is completed most likely due to cell movement and migration into the gaps (Randall et al., 1983). It is speculated that the characteristics of this chicken strain may be an analogue for retinitis pigmentosa due to the initial degeneration of a specific region followed by degenerative effects spreading throughout the rest of the retina.

1.5.4. Retinal degeneration (rd) in the Rhode Island Red

One of the first inherited chicken models to be described is the Rhode Island Red retinal degeneration (*rd*) chick. The mutation in this strain seems to be restricted to a single gene. At the molecular level, the photoreceptors are seen to degenerate after one week post-hatch, when there are large decreases in the number of outer segments, increases in the number spaces between inner segments, and the appearance of large spaces in the outer nuclear layer (Ulshafer et al., 1984). After 6 months, there are very few photoreceptor inner segments and nuclei that remain. The degradations are limited mostly to the central retina, causing thinning of the retinal layers. No recordable ERG measurements can be obtained for the *rd* chicks at any stage of development, whereas the non-affected normal chick shows ERG waveforms that resemble normal adult chicks (Ulshafer et al., 1984). The identification of a null mutation in the photoreceptor guanylate cyclase gene, important for phototransduction, within the *rd* phenotype has made this strain of chickens a useful model for Leber congential amaurosis (Semple-Rowland et al., 1998). Note that this strain has a long history of various name

changes from its early days as the *rc* strain from the histological examinations of adult chicks that show lack of photoreceptors (Cheng et al., 1980) to the more well known *rd* strain in which the study revealed a progressive degeneration of the photoreceptors, instead of dysplasia or developmental defects (Ulshafer et al., 1984). More recently, since the mutation has been isolated to a specific gene, a re-designation of the strain to GUCY1* was deemed appropriate to reflect the presence of the null mutation.

1.5.5. Delayed amelanosis (DAM)

Th DAM strain of chicken is characterized by post-natal amelanosis, leading to a loss of pigments in the feathers. Along with the amelanosis, there is high incidence of blindness and it appears to be a result of a defect within the retinal pigment epithelium (RPE). The RPE in the DAM chicks lack any phagocytic activity and when loss of pigmentation occurs in the choroid, phagocytic pigmentation loss advances and affects RPE layer. These symptoms lead to the development of vision defects, which becomes progressively severe at various rates depending on the individual bird (Fulton et al., 1983). It was also shown that the degeneration of photoreceptors could play a role in the visual loss but more so on a secondary level (Fite et al., 1982). The recorded ERGs show a general decrease in amplitudes of the waveforms with the c-wave being more affected than the a-wave, and the a-wave more affected than the b-wave. The ERG patterns parallel the retinal degeneration changes that were seen at the molecular level.

II. INTRODUCTION

Diseases causing retinal damage are one of the major causes of blindness. Studies focusing on hereditary retinal degeneration have revealed five different forms in chicken models. The retinopathy globe enlarged (*rge*) chickens have a recessive inherited condition (Curtis et al., 1987) in which there is an enlargement of the eye globe and progressive retinal degeneration (Inglehearn et al., 2003; Montiani-Ferreira et al., 2003) due to a deletion mutation in the cone β-transducin gene GNB3 (Tummala et al., 2006). Similarly, the blindness enlarged globe (*beg*) chicken strain also displays enlarged globes and chicks are blind at hatch due to an inherited autosomal recessive mutation (Pollock et al., 1982). Progressive retinal deterioration has been illustrated in the retinal dysplasia and degeneration strain (*rdd*) due to abnormalities in retinal pigment epithelium and neural retina (Randall et al., 1983; Pollock et al., 1982). In the retinal degeneration (*rd*) Rhode Island Red strain, a mutation occurs in the photoreceptor guanylate cyclase gene (*GC1*) causing early onset retinal degeneration and an absent electroretinogram (ERG) recording (Ulshafer et al., 1984). Finally, the delayed amelanotic (DAM) strain shows progressive blindness in relation to loss of choroidal melanocytes (Smyth et al., 1981). Studies carried out on these strains of chickens have shown some links between their genetic mutation and human disease. For example, a null mutation to the photoreceptor guanylate cyclase gene in the *rd* phenotype has made it a useful model for Leber congential amaurosis (Semple-Rowland et al., 1998).

Another genetic mutant strain of White-Leghorn chicken, named Smoky Joe (SJ) chickens, displays multiple symptoms such as, but not limited to, cataracts, buphthalmos, iridodonesis, and phthisis bulbi is caused by an inherited mutation resulting in retinal degeneration (Salter et al., 1997). These ocular symptoms vary in degree and severity at hatch.

Typically by 8 weeks of age, all homozygous chickens are completely blind. Both eyes are always affected, although symptoms for each eye are not always the same, and the retina is often detached or disorganized (Salter et al., 1997). However, the mutation responsible for this mutant strain has yet to be identified.

There are seven major types of vertebrate retinal cells that are important for either visual function or retinal support. These retinal cell types, ganglion, horizontal, cone & rod photoreceptor, amacrine, bipolar and Müller glial cells develop from multipotent retinal progenitor cells and are arranged to form the multilayerd structure of the mature retina.

It remains unclear which retinal cell types are affected in the Smoky Joe chicken strain and information about how retinal degeneration progresses in this strain is also sparse. The purpose of this study is to determine the characteristics of the retinal degeneration and the viability of the retinal cell types during embryonic and post-natal development of Smoky Joe chickens. In addition, the electrophysiological functions of the retina are also examined to complement morphological findings.

III. MATERIALS AND METHODS

3.1. Animals

The *SJ* mutation first appeared in a group of pigmented White-Leghorn chickens maintained at the USDA Avian Disease and Oncology Laboratory (ADOL) in East Lansing, Michigan. The progeny from this line was used to establish a colony at the University of Guelph Arkell Research Station (University of Guelph). Using commercial grade incubators and hatchers (Nature Form), eggs were incubated from day 0 to day 18 at 37.5°C with 55% humidity and then transferred to the hatcher set at 75% humidity. Predictions of whether embryos would be blind or sighted were made based on the phenotypic history of the parent chickens. Three blind and three sighted embryos were extracted from the eggs at 5 time points: embryological day 4 (E4), embryological day 6 (E6), embryological day 8 (E8), embryological day 14 (E14), and embryological day 18 (E18).

SJ chicks typically hatch on day 22. Post-hatch chicks were sacrificed at time points: day 1 (D1), week 1 (W1), week 2 (W2), week 3 (W3), week 4 (W4), week 5 (W5), week 6 (W6), week 7 (W7), week 8 (W8) and week 9 (W9). Samples from three blind and three sighted chicks were obtained for each time point listed.

3.2. Tissue extraction

In embryos at E4 and E6, eyes were too small to be enucleated. To avoid damage, whole embryos were removed from the eggs and fixed in 4% (w/v) paraformaldehyde in Sorensen's phosphate buffer (SB: pH 7.5) solution for 20 mins. Embryos were then washed three times in SB and then cryoprotected in 30% (w/v) sucrose in SB overnight. Embryos were embedded in Optimal Cutting Temperature Embedding Medium before being frozen. At E8 and E14, embryonic eyes were large enough to be enucleated but they remained too small for dissection.

Therefore, entire globes were processed (fixed, washed, and cryoprotected). Only eyes from E18 chicks were large enough for the eyecup to be extracted. For post-hatch chicks, the eyes were extracted for all time points. Once these eyes were enucleated, incisions were made equatorially at the ora serrata and the anterior segments, containing the lens and cornea, were discarded. The remaining eyecups, containing the retina, choroid and sclera were processed as above before being frozen. All the tissue samples were sectioned at 12 µm, and mounted onto Superfrost Plus glass slides (Fisher Scientific). Sections were allowed to air-dry before being stored at -20°C. Transverse sections were obtained for whole embryos while cross sections were obtained for the globes and eyecups. Only the left eyes were analyzed.

3.3. Immunohistochemistry

Only central sections of the retina of embryo and post-hatch chicks were used for immunohistochemical processing. Sections were washed (3 x 5 min) in phosphate buffered saline (PBS: 137 mM NaCl, 3 mM KCl, 101 mM Na_2HPO_4, 2 mM KH_2PO_4, in deionized water) and permeabilized with 0.1% (v/v) Triton-X in PBS (30 min at room temperature; RT). Slides were washed again (PBS, 3 x 5 min). Non-specific binding was prevented by incubating slides with 4% (w/v) bovine serum albumin (BSA) in PBS for 30 min at RT. Primary antibodies against several specific markers were used: mouse anti-Brn3a (1:200, Chemicon [Millipore], MAB1585; ganglion cells), mouse anti-Ap2α (1:200, Developmental Studies Hybridoma [DHSB], 3B5; amacrine cells), mouse anti-glutamine synthetase (1:100, BD Biosceinces, 610517; Müller cells), mouse anti-protein kinase C (1:200, Sigma-Aldrich, P5704; bipolar cells), rat anti-Lim1+2 (1:10, DHSB, 4F2; horizontal cells), mouse anti-visinin (1:200, DHSB, 7G4; early cones), wheat germ agglutinin lectin (1:100, EY Laboratories, R-2101-5; rods) and anti-rhodopsin kinase 1A (1:200, Thermo Scientific, MA1-720; rods and

cones). All primary antibodies were applied to slides and, except for anti-Lim1+2, incubated at 37°C for 2 hours in a humidified chamber. Primary antibody Lim1+2 required incubation overnight at 4°C.

After washing (PBS. 3 x 5 min), secondary antibodies anti-mouse IgG Fab specific conjugated to Fluorescein Isothiocyanate (FITC) or anti-mouse IgG Fc specific conjugated to Tetramethyl Rhodamine Isothiocyanate (TRITC) (both 1:200, Sigma-Aldrich, F5262 and T6653, respectively) were applied and incubated at 37°C for 1 hour. Slides then were washed (PBS, 3 x 5 min) and counterstained with 1 M 4',6-diamidino-2-phenylindole (DAPI, 5 min) to label cell nuclei. Slides were washed again (PBS, 3 x 5 min) before being mounted with Prolong Antifade Gold (Invitrogen) and covered with a coverslip. For negative controls, serum and secondary antibodies were applied to sections with no primary antibody.

3.4. Imaging

Microscopy and imaging analysis were performed using an upright fluorescence deconvolution microscope (Zeiss Axio Imager.Z2). Images were obtained at 20x magnification resulting in a field of view with a diameter of 450 µm and retinal lengths measured at an average of 464 µm. Z-stacked images were collected to allow for ease of counting.

3.5. Cell counts and Analysis

Images of the central region of the retina for each sample were used for cell counts. The total numbers and the numbers of the specific retinal cell types were counted in the two neuroblastic layers, the outer neuroblastic layer (ONBL) and the inner neuroblastic layer (INBL) in younger embryos (E4-E8), and the three nuclear layers, the outer nuclear layer (ONL), the inner nuclear layer (INL) and the ganglion cell layer (GCL) for the older embryos (E14-E18) and for the post-hatch chicks. The cells of the ONL and GCL layers were counted across the retinal

lengths for each image. For the INL, five 10 μm wide rectangular boxes were superimposed on the images of this layer and cells within the boxes were counted. The total number of INL cells across the retinal lengths of the image was then calculated. For each retinal cell type, the cells were all counted in full across the entire retinal lengths. Average cell counts were determined for three blind (n=3) and three sighted (control, n=3) SJ birds at each time point. The averages of the total number of cells, the averages of the cell count means per nuclear layer, and the averages and percentages of the specific cell types means were statistically analyzed with two-way ANOVAs and Tukey post-hoc tests to further determine significant differences between the blind and sighted SJ chickens. Values were considered significant at $p \leq 0.05$.

3.6. Animals for ERGs

Newly hatched SJ chicks were kept at the University of Guelph Arkell Research Station for 1 week to gain strength. 13 chicks (n=5 blind and 8 sighted) were then transferred to the University of Waterloo where they were floor housed in the Optometry building. At W2, the ERG measurements were started on both the blind and sighted birds, continuing on a weekly basis until W9.

3.7. Pre-ERG setup

All birds were first dark adapted for 20 mins. Once dark adapted, one drop of proparacaine (topical anesthetic) was applied followed by a 4 mins wait for the anesthetic to take effect. After the 4 mins wait, one drop of 5 mg/ml vecuronium bromide (VB: pupillary dilator), in a 1% methylcellulose (inert viscous agent) and 0.13% benzalkonium chloride (preservative) mixture, was administered. VB drops were repeated every 4 mins until the pupils were seen to be dilated. In between each drop, the chicken were placed back into an enclosed boxed, with

air holes, maintained at a constant temperature range of 39-41°C using a heating pad.

The breast muscle of the chicken was wiped down with sterile antiseptic alcohol pads. The chickens were injected intramuscularly with a mixture of ketamine (0.533 ml/kg) and xylazine (0.266 ml/kg). The chickens were allowed to rest until they became anesthetized (*i.e.* when they did not not move/respond upon prodding) after which their body temperatures were recorded using a rectal temperature probe lubricated with a sterile lubricant. The internal body temperature of these SJ chickens is 42°C and was maintained by wrapping the chicken in a small blanket for the duration of the ERG in addition to a water heated platform (38°C or 42°C) on which the anesthetized birds were placed. A head holder on the platform stabilized the chickens' head and lid retractors kept the eyelids open. One drop of artificial tears (Celluvisc) was administered to each eye to maintain moisture on the cornea after the placement of lid retractors.

3.8. ERG protocol and post-ERG

Corneal loop electrodes were placed on the surface of each cornea of the anaesthetized bird. The head was wiped down with sterile alcohol pads where a ground needle electrode was inserted under the skin. The Ganzfeld stimulators (Diagnosys LLC, Massachusetts), were placed 5 cm in front of each chicken eye and kept at a constant uniform field of white light. The protocol stimuli consisted of 4 ms light flashes that were separated by 20 s dark intervals. The intensity of each light flash increased in half-log steps from 0 cd.m/s^2 to the maximum intensity of 31.62 cd.m/s^2. Following the ERG recordings, the chickens were allowed to recover in the heated box. The majority of the procedures were non-invasive except for the rectal temperature probes and the needle electrodes.

3.9. Analysis of ERG data

To assess the retinal function of blind birds compared to that of sighted birds, two principle measures of the ERG waves were analyzed (Figure 2). The amplitude for the a-wave was taken as the absolute voltage change measured from the baseline to the first negative trough and the a-wave implicit time was measured from the onset of the light stimulus to the trough of the a-wave. The b-wave amplitude was measured as the absolute value of the difference between the a-wave trough to the b-wave peak. Implicit times for the b-wave were measured from the onset of the light stimulus to the b-wave peak (Figure 2).

Oscillatory potentials (OPs) were extracted from the raw ERG recordings using Fast Fourier Transform band-passed with low and high filters between 75 to 300 Hz in Sigma-Plot (ISCEV; Marmor et al., 2004). OP amplitudes were measured in the same manner as a- and b-wave amplitudes, with the absolute values of the difference between the previous OP troughs to the OP peaks. Implicit times were taken from the onset of the stimulus to the OP peaks.

Amplitudes and implicit times were statistically analyzed using repeated measure ANOVA with a Greenhouse-Geisser correction with $p \leq 0.05$ considered significant.

IV. RESULTS

4.1. Embryonic development of the retina in Smoky Joe chickens

4.1.1. The total number of cells within nuclear layers during development is reduced in blind animals

At the first embryonic time point for which samples were collected (E4), there was already a difference in total retinal cell number between the blind and sighted birds, though not significantly (E4, blind vs sighted: 195556±9347 vs 211018±14285 cells/mm^2, p=0.9958). This trend was maintained throughout all the rest of the embryonic time points, where blind SJ embryo retinas contained a significantly lower number of cells in total compared to sighted SJ embryos across all time points ($p<0.0001$). Although retinas of blind embryos had fewer cells, the development and proportional increase in the number of retinal cells across all time points showed a similar trend for both blind and sighted (Figure 3). There was a continuous increase in cell growth up until E8 when the number of cells began to plateau in both blind and sighted eyes (Figure 3). At the last stage of development that tissues were extracted (E18), the total number of cells in the blind SJ embryos was significantly less than that of the sighted SJ embryos (E18, blind vs sighted: 309156±4075 vs 384986±18651 cells/mm^2, Tukey: p=0.0388).

Two neuroblastic layers were distinguishable at an early stage in development, at E4 based on cell density (Figure 4, E4). Following this point, cells differentiate and migrate towards specified locations in the retina and the neural retina segregates into the three nuclear layers (GCL, INL, and ONL). Qualitative analysis of the images indicated that the nuclear layers began to form around E8 in a number of embryos but not all. Noticeably, the nuclear layers were formed mostly within the sighted SJs, which coincides with normal wild-type chick development (Mey and Thanos, 2000), whereas the development of the nuclear layers in

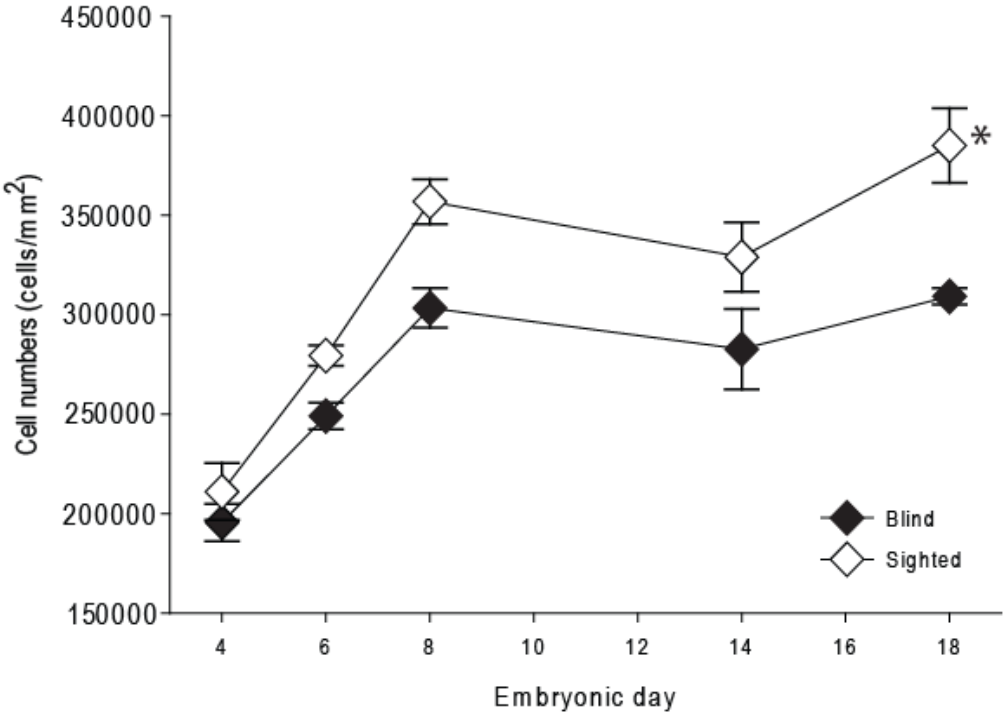

Figure 3. Average total cell counts of retinal cells across all embryonic time points for blind (n=3) and sighted (n=3) Smoky Joe embryos (±s.e.m), ($p<0.0001$). Asterisks (*) denote significant differences between blind and sighted birds at the specific time point.

blind SJs were delayed until E14. At E14, the transformations of neuroblastic layers into the three nuclear layers were formed in all samples from both blind and sighted birds and therefore the cell counts in the three nuclear layers from E14 to E18 were made and compared between blind and sighted birds (Figure 4). The difference in total cell number between the blind and sighted retina was largely due to a loss of cells in the INL in blind birds at E14 and E18 with a significant difference observed at E18 (Figure 5; E18, blind vs sighted: 257500±2626 vs 328796±19827 cells/mm^2, Tukey: $p=0.0388$). In contrast, no differences between the birds was detected for cell numbers neither in the ONL nor in the GCL layers at these later time points (Tukey, E14: $p=0.5263$, $p=0.9999$; E18: $p=0.7010$, $p=0.7787$, respectively).

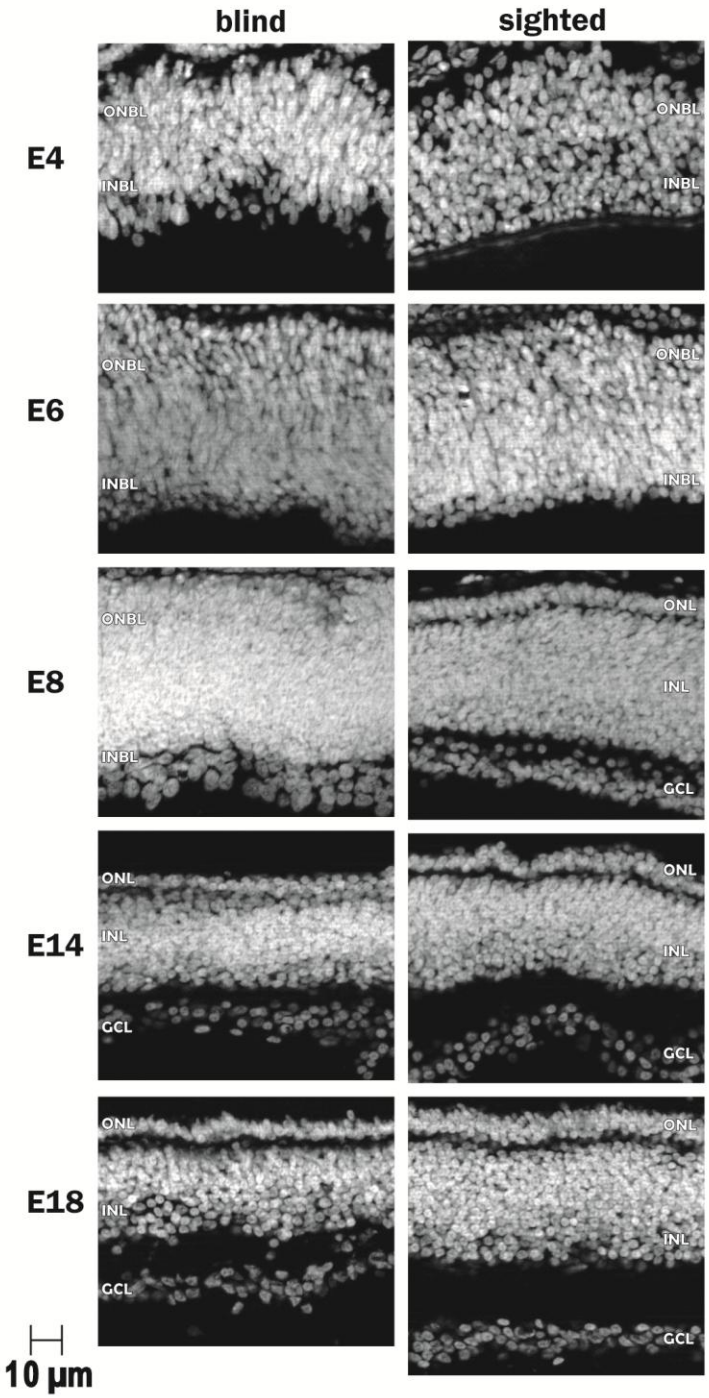

Figure 4. Retinal cells stained with DAPI of blind and sighted SJ embryos across all time points obtained by deconvolution microscopy. ONBL, outer neuroblastic layer; INBL, inner neuroblastic layer; ONL, outer nuclear layer; INL, inner nuclear layer; GCL, ganglion cell layer.

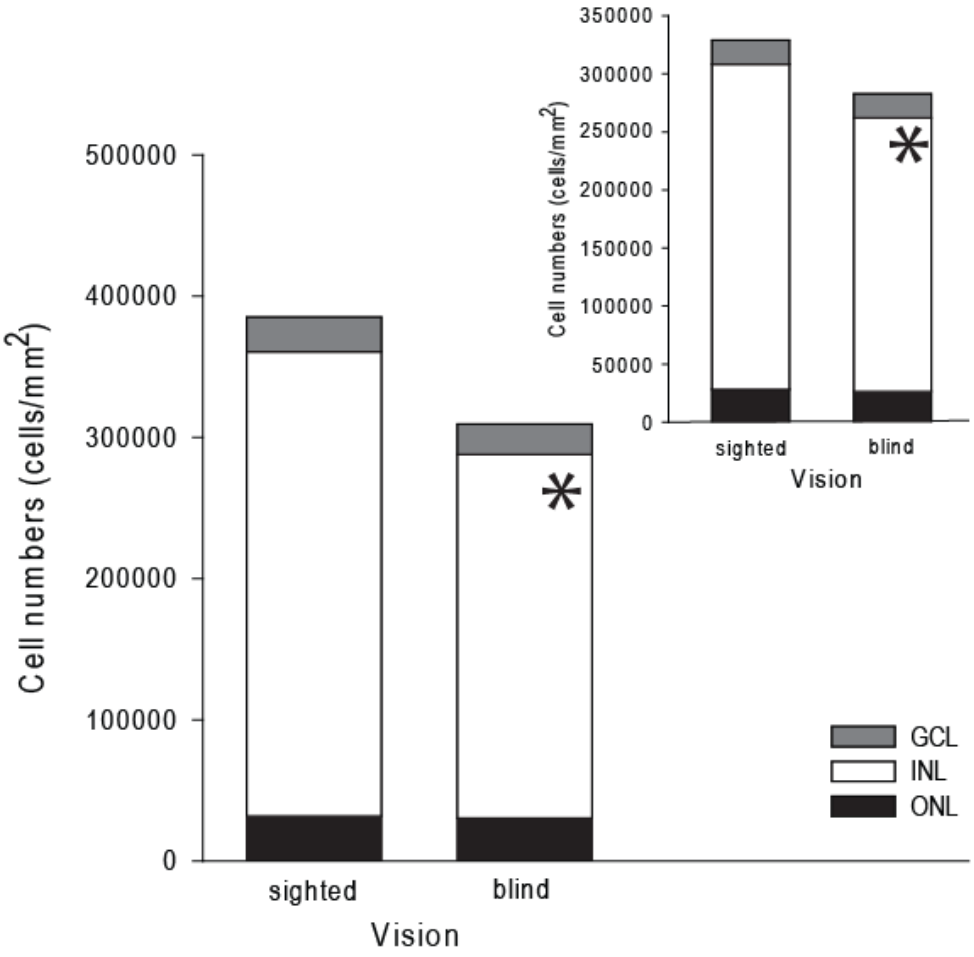

Figure 5. Average total cell counts of retinal cells within the ganglion cell layer (GCL), the inner nuclear layer (INL) and the outer nuclear layer (ONL) for blind (n=3) and sighted (n=3) Smoky Joe embryos at embryonic day 18 (Inset: GCL, INL and ONL average total cell counts for E14). Asterisks denote significant difference between blind and sighted within each layer.

4.1.2. Number of specific retinal cell types differs between blind and sighted animals during embryonic development

The ganglion cell marker Brn3a was first observed in blind and sighted embryos at E8. The number of ganglion cells at this time point was lower in blind embryos (E8, blind vs sighted: 16234±1657 vs 19424±1772 cells/mm^2) but no significant difference was found ($p=0.9998$). Blind SJs displayed slower ganglion cells growth rates and lower numbers compared to sighted

birds for the remaining time points E14 and E18, but once again no significant differences were detected (p=0.9992 and p=0.2498, respectively). Analysis of the overall number of ganglion cells across all the time points showed no significant differences between blind SJ embryos and sighted ones (Figure 6A, p=0.0920) even though there were less cells in the blind birds. Moreover, the percentage of ganglion cells in the retina relative to the total number of cells throughout development was not significantly different between the two visual conditions (Figure 6B, p=0.7462).

Horizontal cells were first detected in both blind and sighted SJ embryos as early as E4 using the marker anti-Lim1+2. For both blind and sighted embryos, a number of horizontal cells were observed in the INBL at early stages and they slowly migrated to the outer edge of the INL at E8. The number of horizontal cells did not significantly differ between blind and sighted birds at these two time points and coincidently, there was no difference in the number of cells overall across all time points (Figure 6C, p=1.0000).

The photoreceptor marker Visinin has been described to be cone specific during embryonic development (Hatakenaka et al., 1985; Yamagata et al., 1990) and was first detected at E6 in blind and sighted embryos in the ONBL. For blind embryos, there was incomplete segregation of the three nuclear layers and therefore cone cells remained in the ONBL whereas they were already in the ONL for sighted embryos. The growth trend of cone cells for blind birds was similar to sighted birds, but at each time point, the number of cone cells was lower in blind compared to sighted embryos. Overall, the number of cone cells across all time points was significantly lower in blind birds (p=0.0003) and time point E14 was the only time point at which a significant difference between blind and sighted (Figure 7A, Tukey: p=0.0434) was detected. However, in terms of the percentage of cone cells in the retina relative to the total

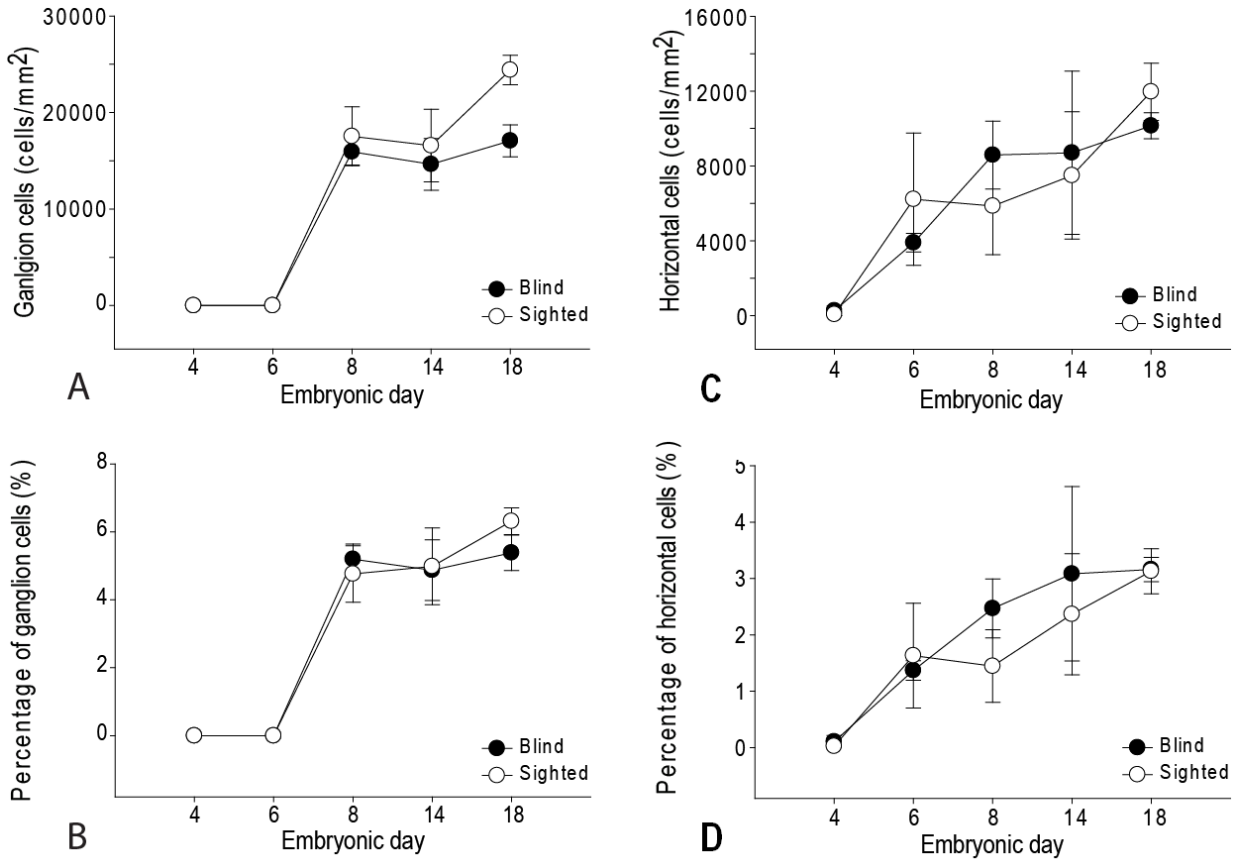

Figure 6. Average counts and percentages of ganglion (A,B) and horizontal (C,D) cells across all embryonic time points for blind (n=3) and sighted (n=3) Smoky Joe embryos (±s.e.m). Asterisks (*) denote significant differences between blind and sighted birds at the specific time point.

number of cells throughout development there was no difference (p=0.9613). The detection of rod cells was quite late in embryonic development, at E18 (Figure 7B) within the ONL. Cell counts showed that there were significantly less rod cells in blind embryos than in sighted ones at this late time point (E18, blind vs sighted: 1039±214 vs2582±162 cells/mm^2, p<0.0001), with the percentage of rod cells relative to the total number of cells throughout development in sighted embryos being significantly double of those within blind embryos (E18, blind vs sighted: 0.40±0.08vs 0.82±0.05%, Tukey: p=0.0002.

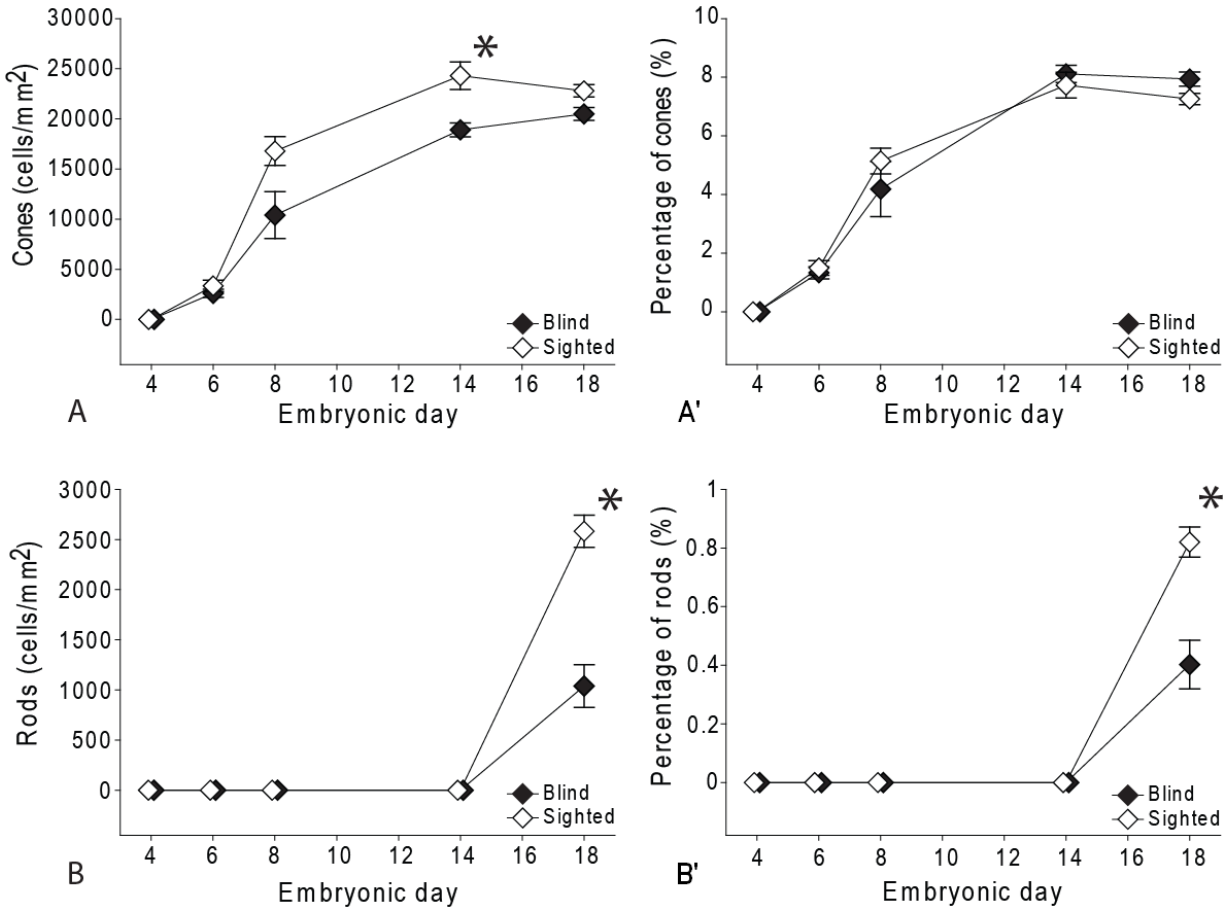

Figure 7. Average counts and percentages of cones (A,A') and rods (B,B') cells across all embryonic time points for blind (n=3) and sighted (n=3) Smoky Joe embryos (±s.e.m). Asterisks (*) denote significant differences between blind and sighted birds at the specific time point.

Interestingly, the specific amacrine cell marker Ap2α was first detected at E6 in only sighted SJ embryos and not in the blind embryos. Detection of amacrine cells in blind embryos did not start until E8, whereas the amacrine cells of the sighted embryos were present in the inner portions of INBL starting at E6, where they continued to increase in numbers and eventually migrated to the INL by E8 (Figure 8). The number of amacrine cells in blind embryos did not stabilize throughout development, in contrast to their sighted counterparts, for which the amacrine cells reached which the amacrine cells reached a plateau around E8 (Figure

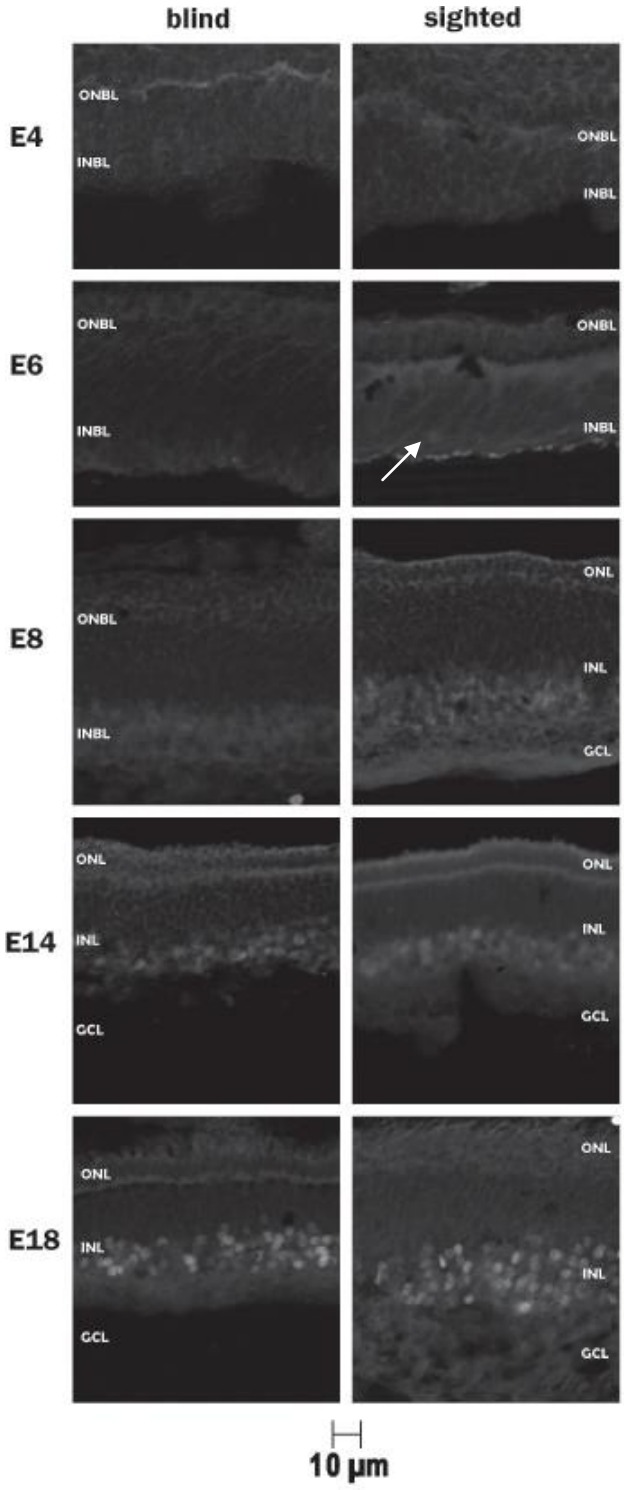

Figure 8. Expression of amacrine cells labeled with anti-Ap2α in cross sections of blind and sighted SJ embryos across all time points obtained by deconvolution microscopy. Arrow indicates initial amacrine cell detection in sighted SJs at E6. ONBL, outer neuroblastic layer; INBL, inner neuroblastic layer; ONL, outer nuclear layer; INL, inner nuclear layer; GCL, ganglion cell layer.

9). In blind SJ embryos at time point E8, there was significantly less amacrine cells compared to sighted embryos (E8, blind vs sighted: 8107±4617 vs 28045±8261 cells/mm^2, Tukey: p=0.0094). In addition, its relative proportion to the total number of retinal cells was also

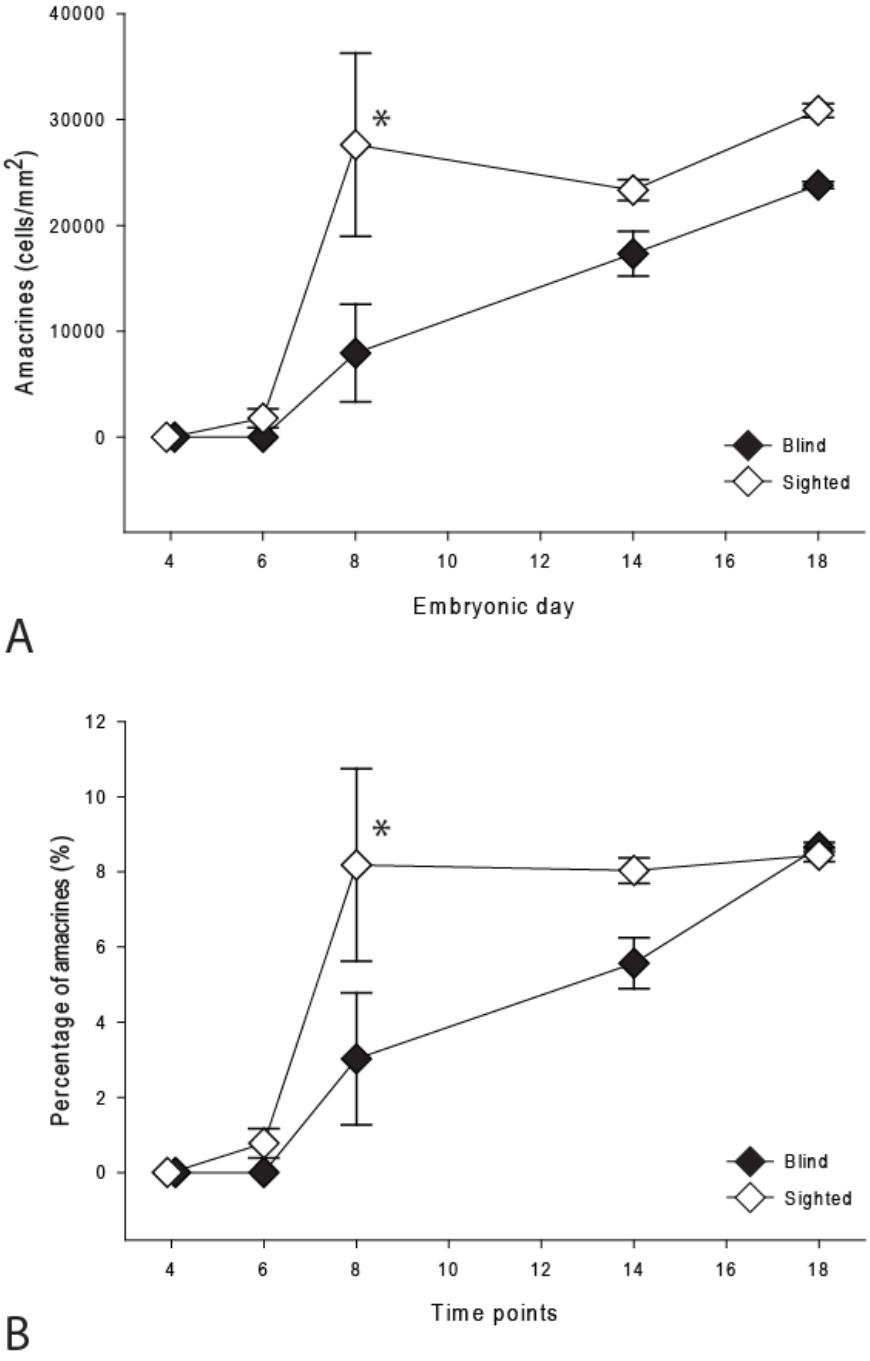

Figure 9. Average cell counts (A) and percentage of amacrine cells (B) across all embryonic time points for blind (n=3) and sighted (n=3) Smoky Joe embryos (±s.e.m). Asterisks (*) denote significant differences between blind and sighted birds at the specific time points.

lower than in sighted embryos (E8, blind vs sighted: 3.08±1.75 vs 8.26±2.43%, Tukey: p=0.0473). In total, there was a significant difference between blind SJ embryos and their sighted controls for the overall number of amacrine cells across all the time points (p=0.0028). Accordingly, the results for the proportion of amacrine cells relative to the total number of retinal cells throughout development were significantly lower for amacrines in blind embryos (p=0.0198).

Both bipolar and Müller cells were only detected at later stages of embryonic development, at E18 in both the blind and sighted SJ embryos. Bipolar cells were observed to have distinct processes that remain within the INL but project towards the ONL and GCL. There was a lower number of bipolar cells in blind embryos but the differences were not significant at the E18 time point (E18, blind vs sighted: 8395±376 vs 12469±2600 cells/mm^2, Tukey: p=0.0539). Similarly, the proportion of bipolars relative to the total number of retinal cells throughout development was not significant (Figure 10B, Tukey: p=0.6879). Müller cells, labeled by the cell marker protein glutamine synthetase (GS), were observed to have processes that span the entire width of the retina through all three nuclear layers. The Müller cell populations between the blind and sighted birds were fairly similar and showed no real difference in number (E18, blind vs sighted: 17325±1697 vs 24033±1410 cells/mm2, Tukey: p=0.2526), nor in the percentage of Müller cells at E18 (Figure 10D, Tukey: p=0.2526). Both bipolar and Müller cell numbers and proportions were not significantly different between blind and sighted SJ embryos throughout embryonic development (bipolar number, percentage: p=0.1327, p=0.4131; Müller *c.f.*: p=0.9330, p=0.2476).

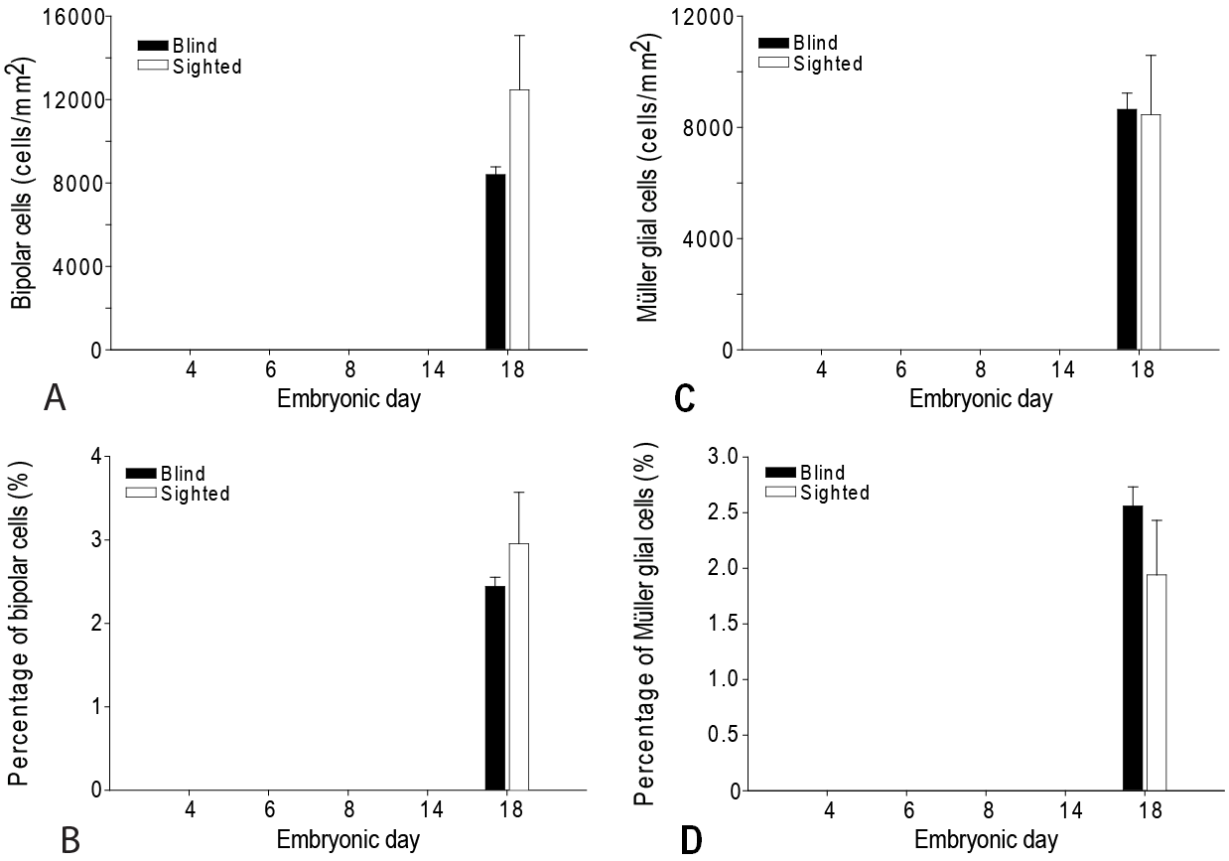

Figure 10. Average counts and percentages of bipolar (A,B) and Müller (C,D) cells across all embryonic time points for blind (n=3) and sighted (n=3) Smoky Joe embryos (±s.e.m). Asterisks (*) denote significant differences between blind and sighted birds at the specific time point.

4.2. Retinal degeneration of post-hatch SJs

4.2.1. Nuclear layer cell numbers less in blind birds throughout post-hatch

SJs hatched at embryonic day 22 and 1 day after hatch (D1), the number of total retinal cells was observed to be at an average of 395792±421 cells/mm^2 in blind and 449054±29814 cells/mm^2 in sighted. These numbers are more than the total numbers at E18 for both blind and sighted birds, but the cell numbers are still less in blind birds compared to sighted birds. The total number of retinal cells in blind birds started to significantly decrease as early as W1 (W1, blind vs sighted: 361348±14629 vs 464046±28046 cells/mm^2, Tukey: p=0.0440) and reached a

low point at W6 (W6, blind vs sighted: 235209±17032 vs 412438±11912 cells/mm^2, Tukey: p=0.0.0003) at which the cell numbers were never able to recover (Figure 11). The changes in number coincide with qualitative observations of thinning of retinas in blind birds starting at W1-W2 timepoints. In contrast, sighted SJs maintained a relatively constant total number of retinal cells throughout the time points examined for post-hatched, although there was a slight decrease at W7. From W1 to W9, there were significant differences in number of cells between blind and sighted overall ($p<0.0001$) and at almost every point.

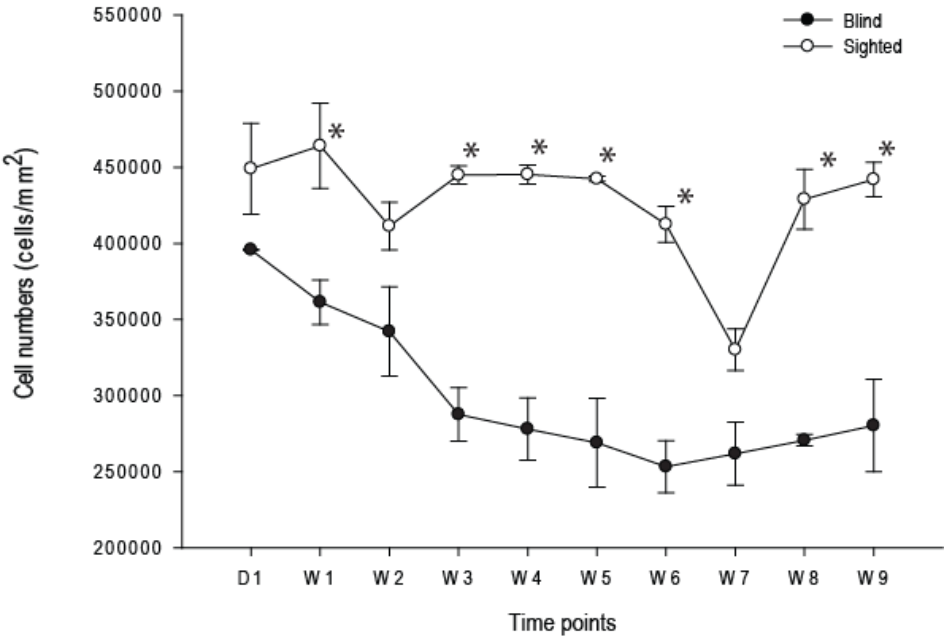

Figure 11. Average total cell counts of retinal cells across all post-hatch time points for blind (n=3) and sighted (n=3) Smoky Joe embryos (±s.e.m), ($p<0.0001$). Asterisks (*) denote significant differences between blind and sighted birds at the specific time point.

Once again, cell counts were obtained for each nuclear layer to determine the region of cell loss. The most significant difference was observed within the INL of the retina, which is consistent with what was found during embryonic development. The blind SJ birds had significantly less cells in the INL throughout post-hatch growth, whereas the number of INL

cells of sighted SJs remained relatively constant (Figure 12). Cell numbers in the INL were lowest in blind birds at W6 with a total of 203518±15786 cells/mm2, whereas in sighted birds at W6, the cell number was 348148±11092 cells/mm2 (W6, Tukey: p=0.0002). It was observed that the ONL was also significantly different between blind and sighted SJs throughout post-hatch growth (Figure 13), where significantly less ONL cells were counted in blind birds starting at W3 (W3, blind vs sighted: 26307±2120 vs 38668±376 cells/mm2, Tukey: p=0.0048). From W3 onwards, cell numbers within the ONL of blind birds were relatively constant across all time points collected, with a significant difference at W6 (W6, blind vs sighted: 27286±2095 vs 38416±529 cells/mm2, Tukey: p=0.0176). Statistical analysis

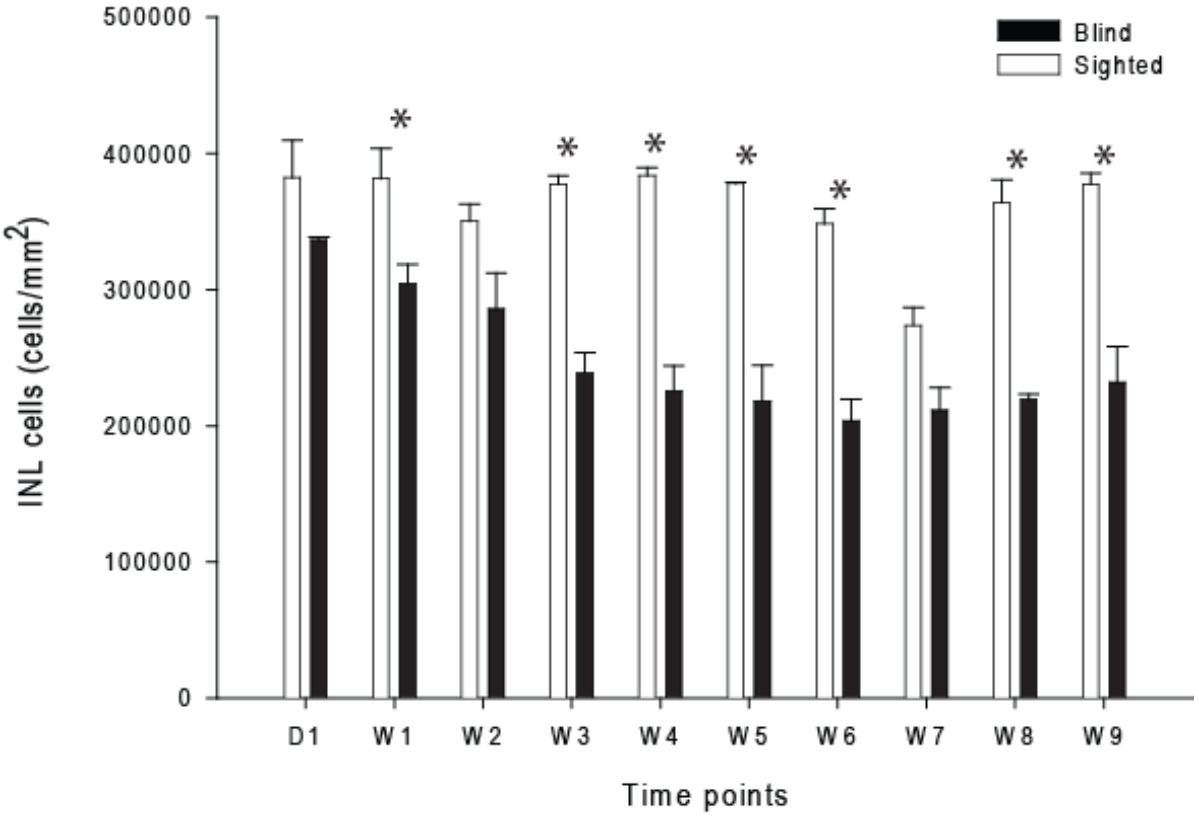

Figure 12. Average total cell counts of retinal cells within the inner nuclear layer (INL) for blind (n=3) and sighted (n=3) post-hatch SJs (±s.e.m) across all time points (p<0.0001). Asterisks (*) denote significant differences between blind and sighted birds at the specific time point.

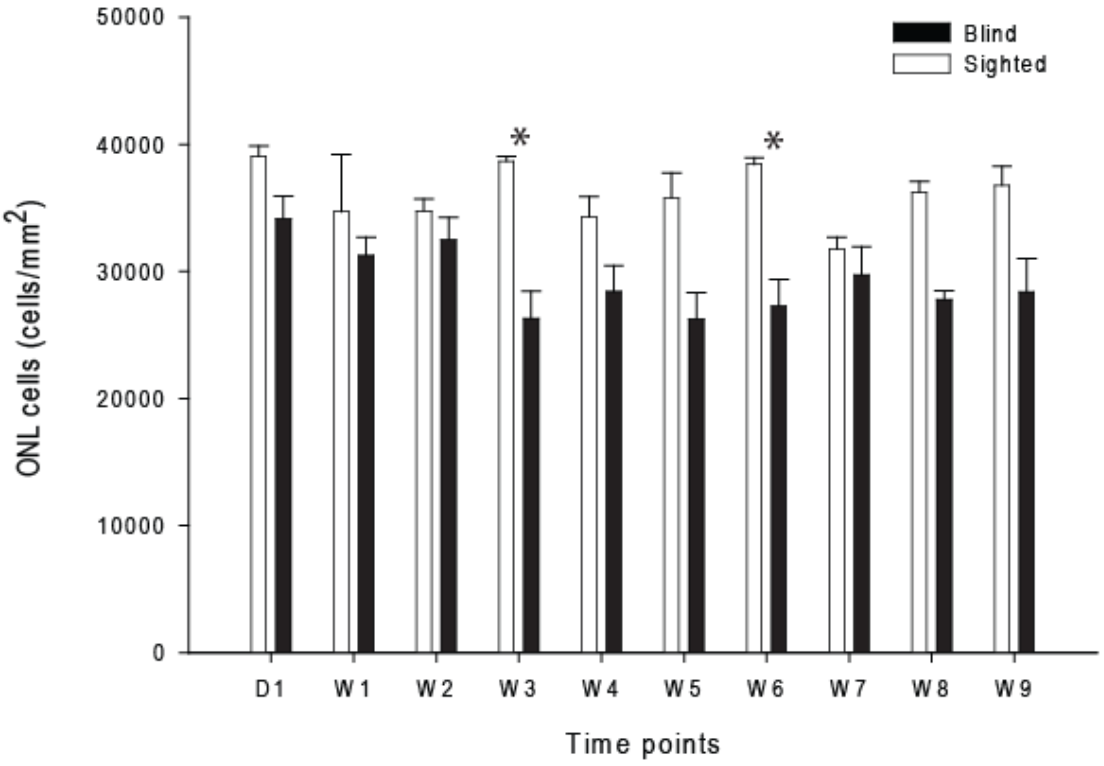

Figure 13. Average total cell counts of retinal cells within the outer nuclear layer (ONL) for blind (n=3) and sighted (n=3) post-hatch SJs (±s.e.m) across all time points ($p<0.0001$). Asterisks (*) denote significant differences between blind and sighted birds at the specific time point.

on counts of the final GCL revealed significant differences between blind and sighted birds throughout post-hatch growth ($p<0.0001$), but only at the very last age observed (W9) was there evidence of a difference at a specific time point (blind vs sighted: 19787±2116 vs 28169±1793 cells/mm^2, Tukey: $p=0.0099$). Differences in the GCL were not seen from any other time point between blind and sighted SJs.

4.2.2. Decrease numbers of specific cell types in post-hatch retinas

The overall counts of ganglion cells labeled with the marker for Brn3a revealed a significant difference between blind and sighted birds across all the post-hatch time points in terms of ganglion numbers (Figure 14A, $p=0.0001$). Within the GCL layer, ganglion cell numbers were

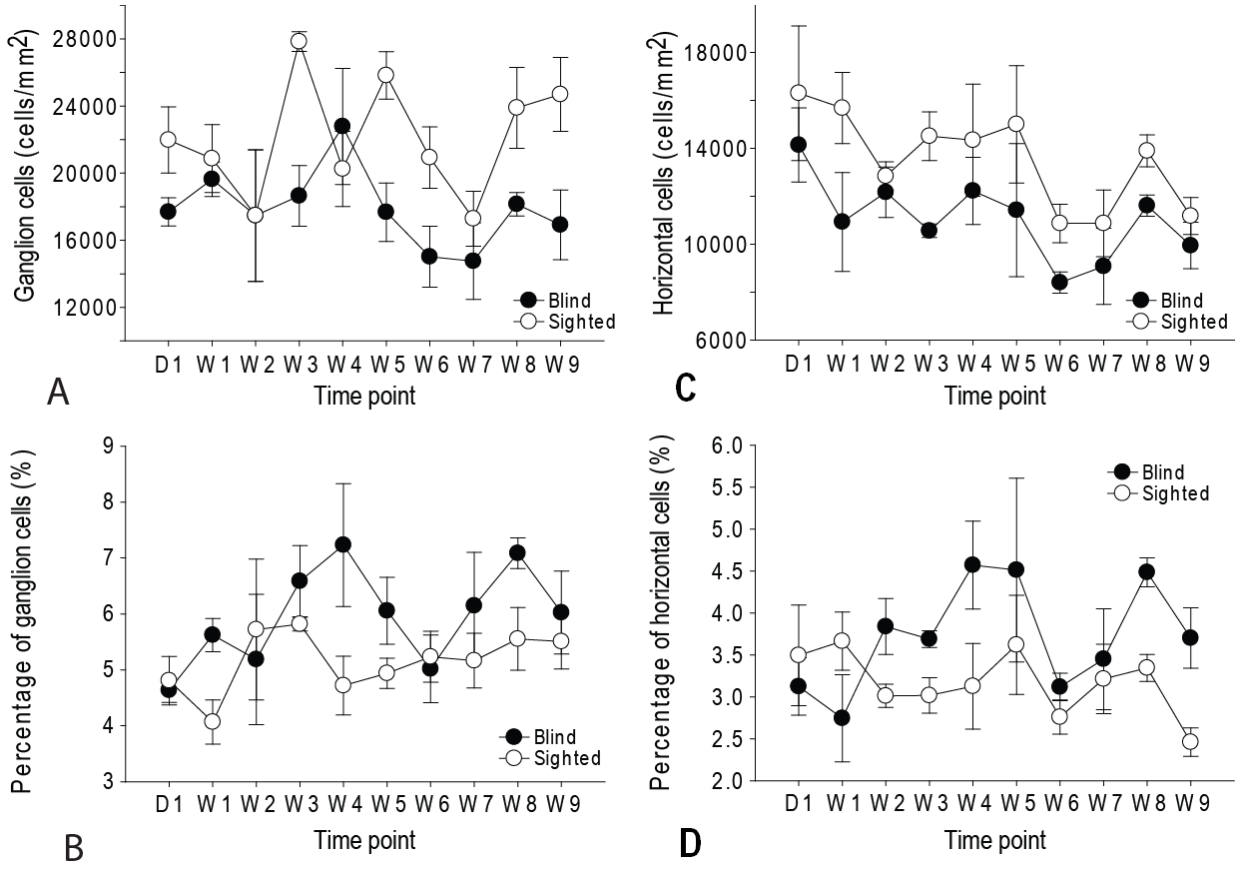

Figure 14. Average counts and percentages of ganglion (A, B) and horizontal (C,D) cells across all post-hatch time points for blind (n=3) and sighted (n=3) Smoky Joe embryos (±s.e.m). Asterisks (*) denote significant differences between blind and sighted birds at the specific time point.

less in blind than sighted birds for most of the time points seen but specifically at each time there was no significant difference. In contrast, when the percentages of ganglions were analyzed, that revealed that throughout post-hatch, proportions of ganglion cells were significantly higher in blind than sighted birds (Figure 14B, p=0.0091). Overall, there was no significant difference in ganglion cell proportions between blind and sighted at any certain time point

. In post-hatch chicks, horizontal cells were detected on the outer surface of the INL forming a row of cells. The average number of total horizontal cells across all time points

were significantly different however in the blind birds compared to that of the sighted birds (Figure 14C, p=0.0008). Similarly to the ganglion cells, the percentage of horizontal cells relative to the total number of cells was significantly higher in blind birds compared to sighted birds (Figure 14D, p=0.0083). Although this was the case for the overall percentage across all the time points, at specific time points there was no significant difference between the blind and sighted birds in terms of total numbers.

Visinin-negative rhodopsin kinase-labelled (VnRK)-cells were calculated as the remainder of the rhodopsin kinase-labelled cells minus visinin-positive cells. The number of visinin-postiive cells were significantly different between blind and sighted birds throughout all post-hatch time points observed (p=0.0002) but at specific time points there were no difference found. Overall at each time point, the number of visinin-positive cells within the blind birds is consistently less than that of the sighted birds. Similarly to previous findings for ganglion and horizontal cells, the percentage of visinin-positive cells relative to the total number of cells indicate a significant difference across all time points (p=0.0020) with blind birds having a higher proportion of cells compared to sighted birds. Although the number and percentages fluctuate slightly, VnRK show significant differences between blind and sighted SJs overall across all the time points in terms of cell number (p=0.0037) and proportions (p=0.0050) but there were no significant differences at the various time points (Figure 15). The average total number of VnRK cells throughout the time points in blind birds is less than sighted birds (blind vs sighted: 1074±2503 vs 8839±5022 cells/mm^2). In addition, the average percentage of VnRK cells relative to the total number of cells across all time points, calculated by taking the average of the percentage of rods for each time point, was also lower in blind birds compared to sighted (blind vs sighted: 2.21±1.29% vs 0.18±0.91%).

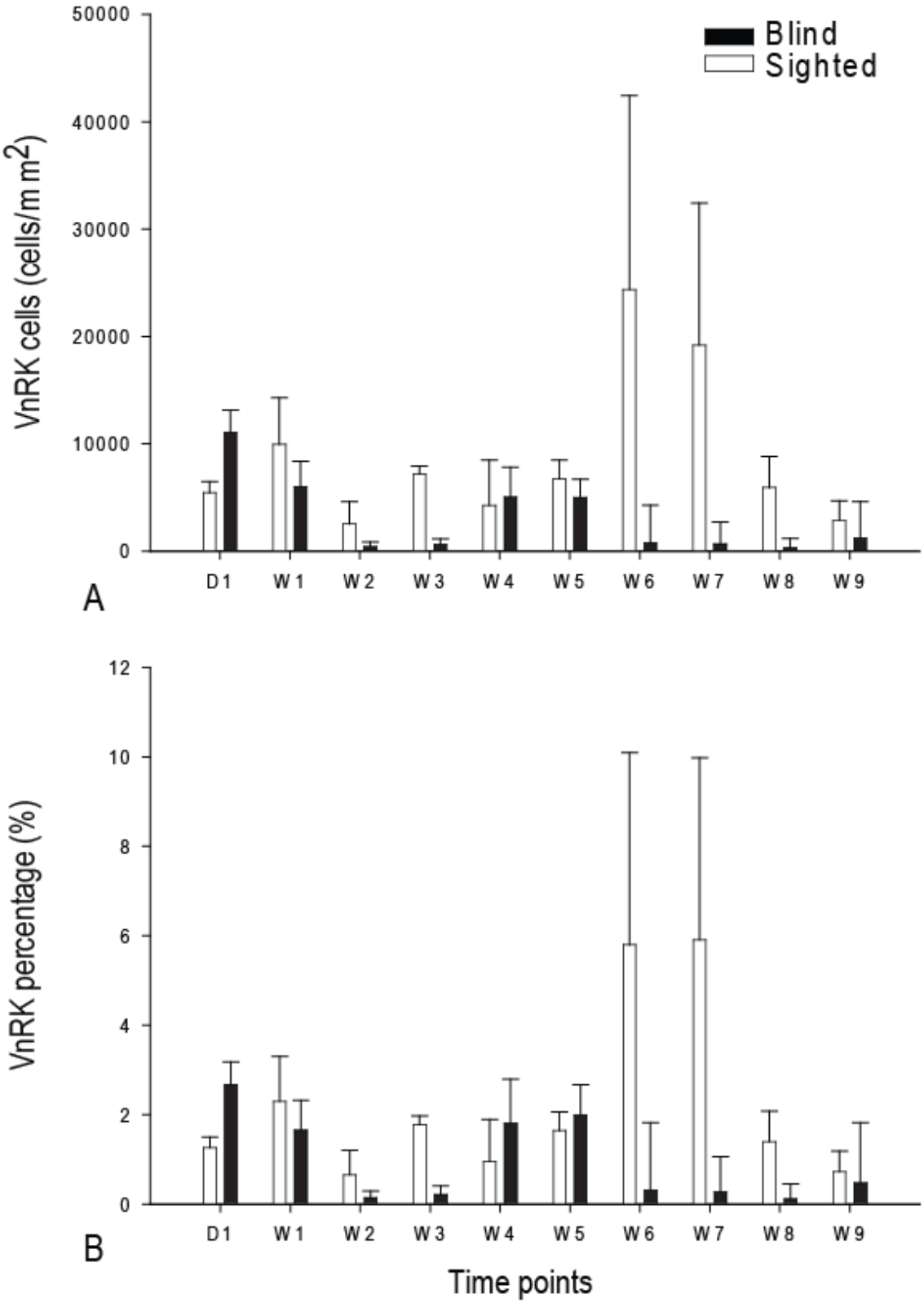

Figure 15. Average cell counts (A) and percentage (B) of rod cells across all post-hatch time points for blind (n=3) and sighted (n=3) Smoky Joes (±s.e.m).

Amacrine cells were detected within the inner portion of the INL layer and contributed to a large portion of the INL cell population (Figure 16). Previously, the amacrine cells in embryonic SJ chicks were found to be significant in terms of the number of cells and its proportions throughout embryonic development. For post-hatch chicks, significant differences between blind and sighted were also observed for overall amacrine cell numbers ($p<0.0001$) and proportions of amacrine cells relative to the total cell numbers ($p=0.0044$) across all time points. The amacrine cells were the only cell types to have significant differences of cell numbers at specific time points between the blind and sighted birds (Figure 17). However, the percentage of amacrine cells relative to the average total number of cells at the various time points did not.

Bipolar and Müller cell numbers were not significantly different between blind and sighted birds throughout post-hatch time points (Figure 18, $p=0.1174$, $p=0.1089$, respectively). In terms of proportion, both these cell types showed significant differences (Figure 18, bipolar: $p=0.0105$, Müller: $p<0.0001$) as total retinal cell numbers decreased. For various time points, only Müller cells showed a significant difference at W6 in terms of percentage of Müller cells relative to the total number of cells (W6, blind vs sighted: 19.79±2.72 vs 11.40±1.00%, Tukey: $p=0.0094$)

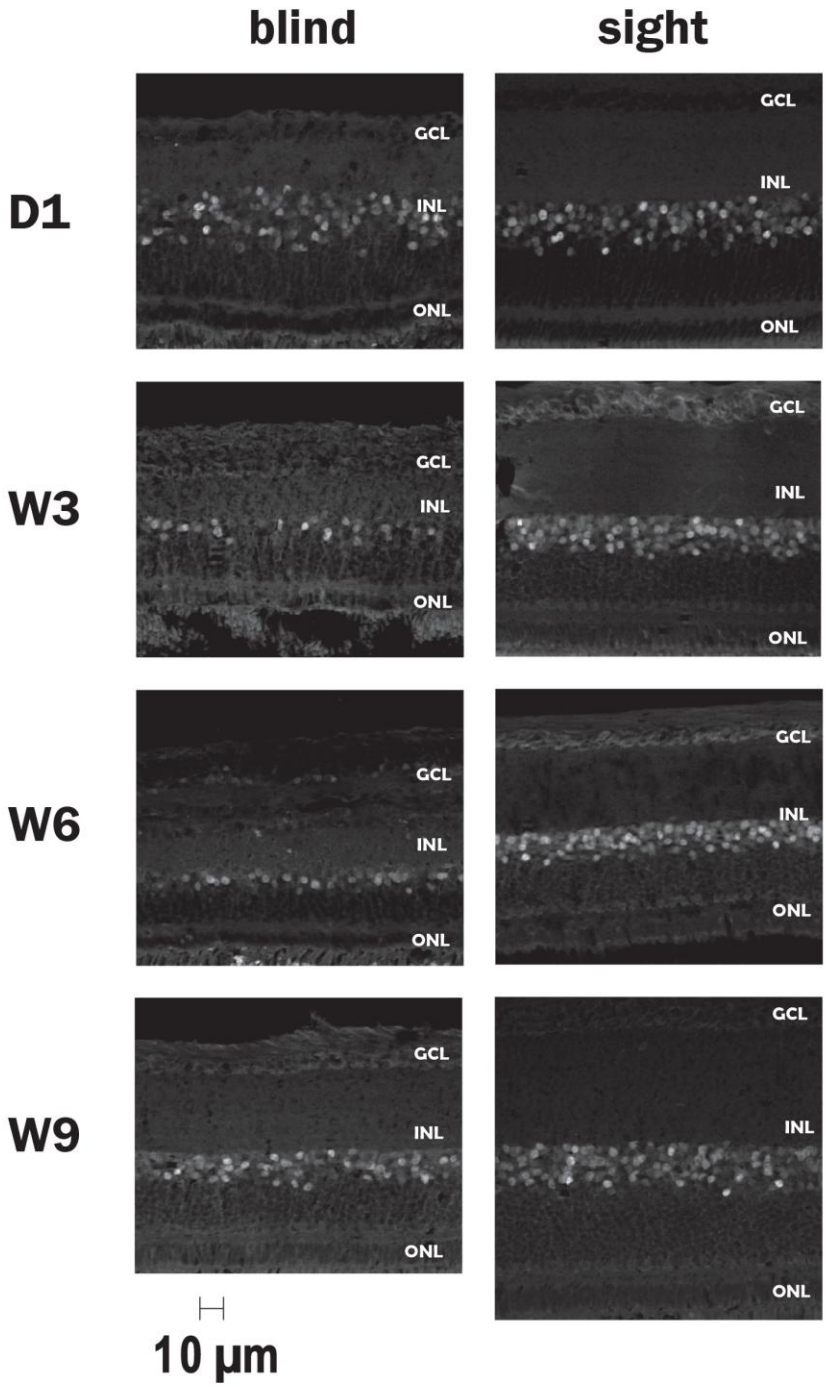

Figure 16. Expression of amacrine cells labeled with anti-Ap2α in cross sections of blind and sighted post-hatch SJs across beginning, middle and end time points obtained by deconvolution microscopy. ONL, outer nuclear layer; INL, inner nuclear layer; GCL, ganglion cell layer.

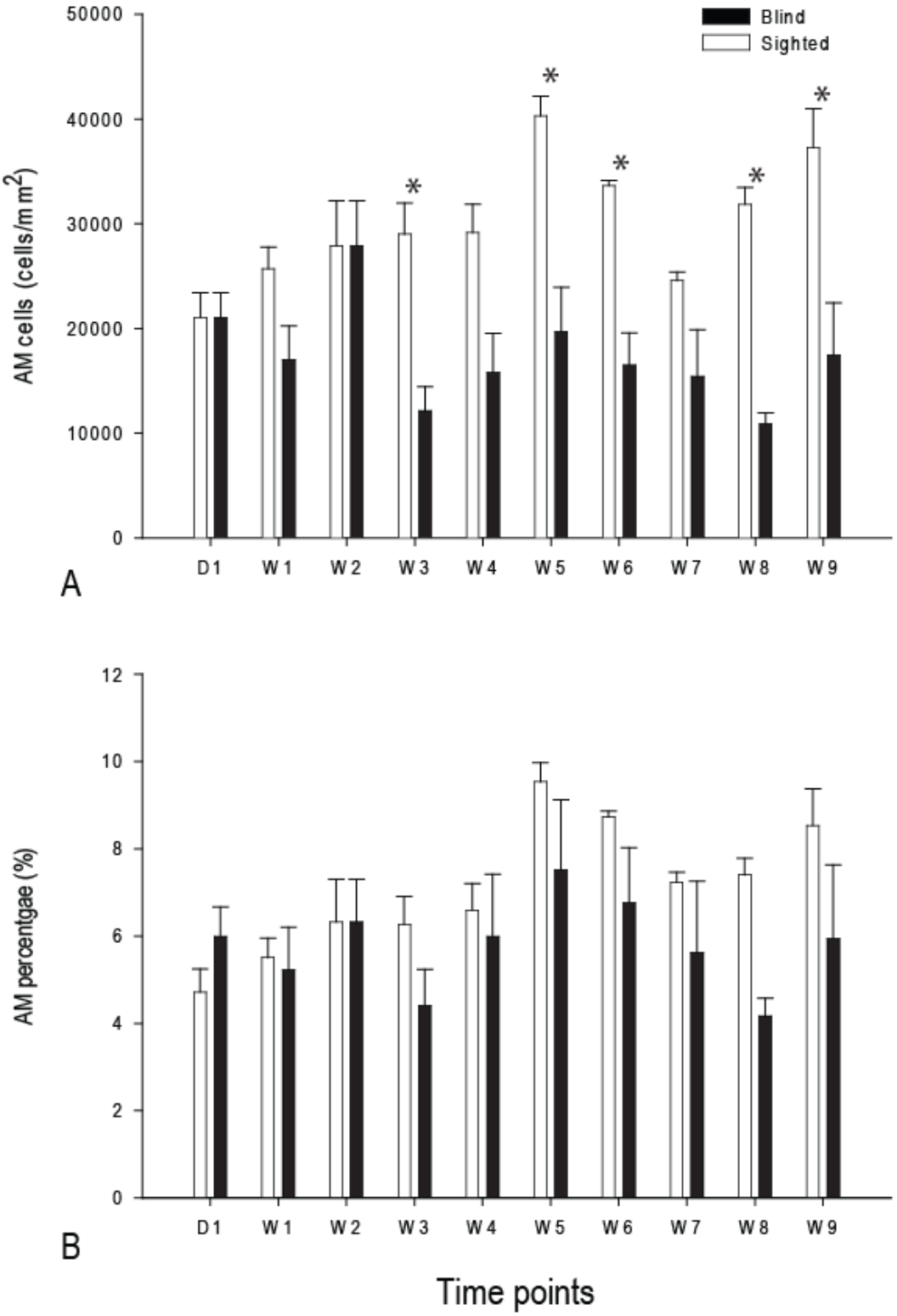

Figure 17. Average cell counts (A) and percentage (B) of amacrine cells across all post-hatch time points for blind (n=3) and sighted (n=3) Smoky Joe embryos (±s.e.m). Asterisks (*) denote significant differences between blind and sighted birds at the specific time points.

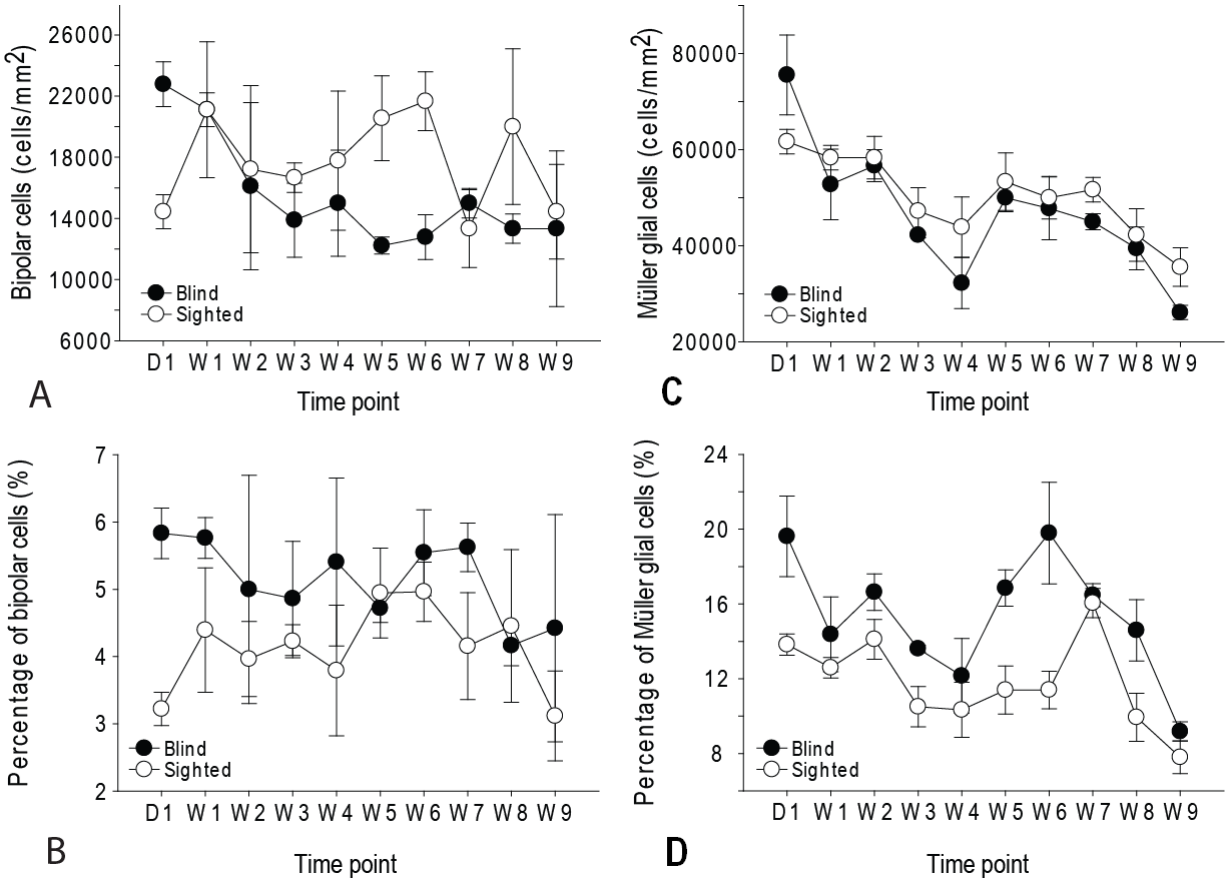

Figure 18. Average counts and percentages of bipolar (A,B) and Müller (C,D) cells across all post-hatch time points for blind (n=3) and sighted (n=3) Smoky Joe embryos (±s.e.m). Asterisks (*) denote significant differences between blind and sighted birds at the specific time point.

4.3. ERG measurements

Samples of dark-adapted flash-ERG waveforms recorded for blind and sighted SJs, as well as for a sighted bird that progressively developed blindness, dubbed "Partially-sighted", are shown in Figure 19. This latter bird was discovered to be partially sighted only after ERG measurements were taken. Previously, observations of behavior showed that the bird was blind. The waveforms for sighted SJs were comparable to other normal sighted chicken ERG measurements (McGoogan and Cassone, 1999). The difference is seen in the blind SJs where blindness at W5 abolishes the ERG response. Blind chicks from hatch showed abolished ERG

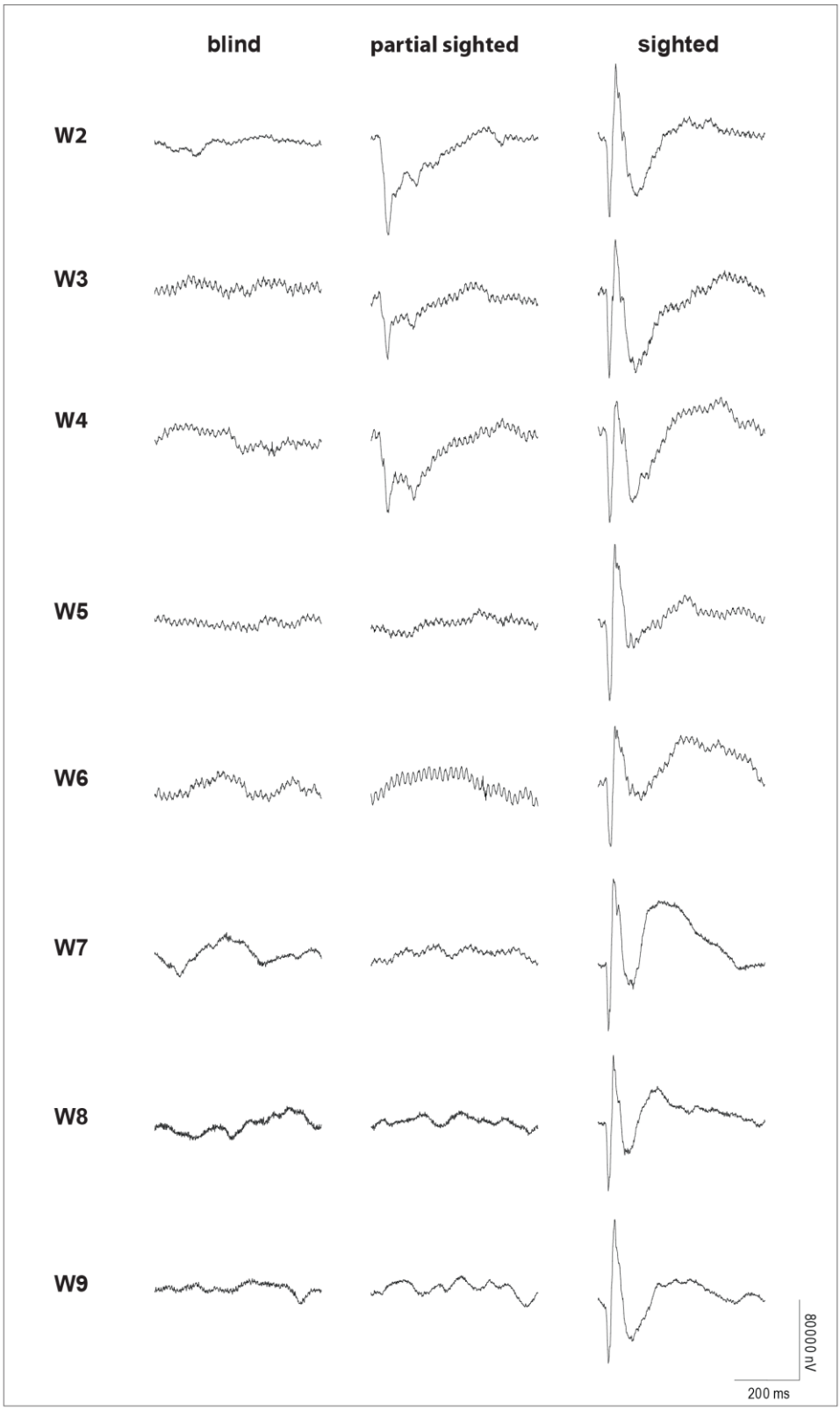

Figure 19. Representative sample of ERG recordings from blind, partially sighted and sighted SJs across all recorded post-hatch time points.

responses from the start of the ERG recordings at W2. For the one chick that is partially sighted, initial waveforms at an early age showed decreased b-wave amplitudes, followed by a progressive decrease of a-wave amplitude, (W2-W4, Figure 19, middle column). Amplitudes and implicit times of the a- and b-waves in the ERGs are shown in Figure 20. Smaller waveforms with a lower slope contributed to the longer implicit times found in blind birds compared to that of sighted birds. Statistical analysis revealed that a-wave amplitudes were significantly smaller within the blind birds compared to the sighted birds at each time point and throughout all the time points ($p \leq 0.05$). In addition, due to the fact that b-waves were scarcely detectable, the b- wave amplitudes of the blind birds were signficantly smaller in comparison to the sighted birds ($p \leq 0.05$). a-wave and b-wave implicit times were not significantly different between blind and sighted birds ($p \geq 0.05$). When completely blind, the ERG

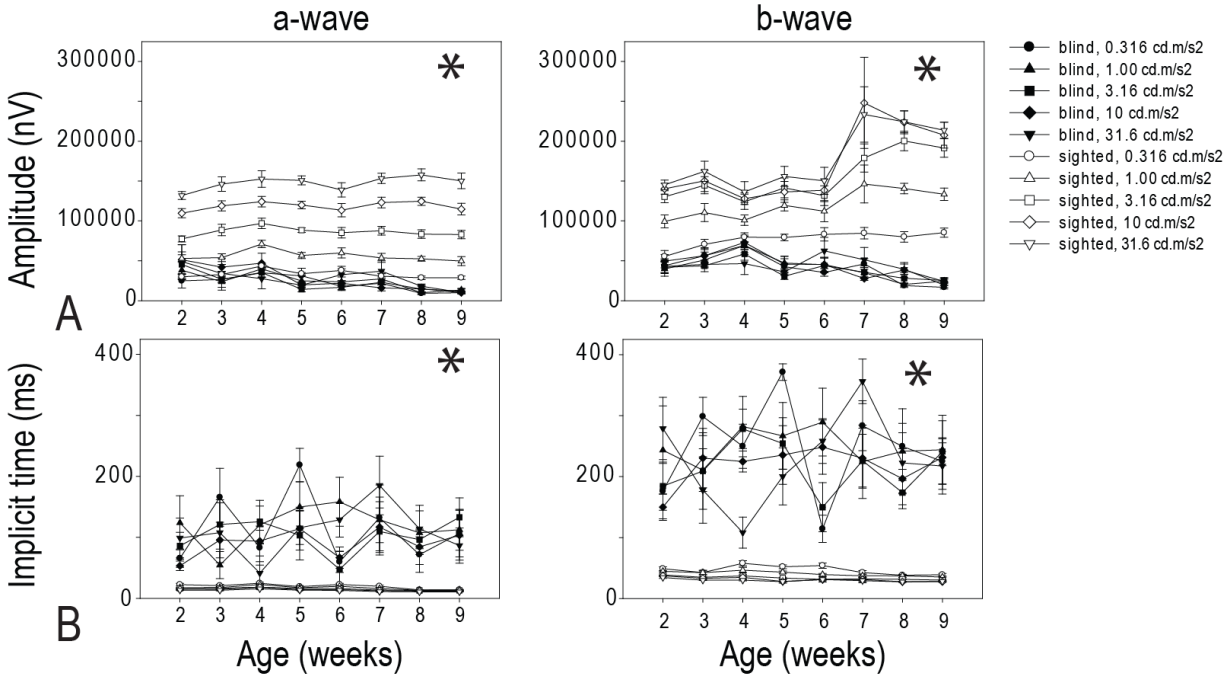

Figure 20. The (A) amplitudes and (B) implicit times of a-waves and b-waves of blind and sighted SJs across all time points recorded. Asterisks denote significant differences between blind and sighted over all post-hatch time points.

waveforms were abolished and undetected. Significant changes in ERG waveforms were not seen in the sighted SJs throughout the post-hatch time points.

4.3.1. Oscillatory potentials (OPs) of SJs

Representative oscillatory potentials (OPs) recorded for both blind and sighted are shown in Figure 21. Notice that in general there were five OP wavelets detected within the sighted birds. Initial observations revealed that the amplitudes of OPs within the blind SJs were significantly lower compared to that of sighted bird. Small OP wavelet amplitudes were detected in the one bird that showed progressive blindness, shown as W2-W4 in Figure 21. Those birds that were completely blind showed even smaller OP amplitudes and OPs were difficult to detect.

Amplitudes for the partially blind were not significantly different from those of blind birds and therefore did not affect the overall outcome OP wavelet amplitude analysis. There were significant differences for each OP at every time point, as well as overall throughout all the time points (Figure 22). The recorded OP amplitudes were far smaller in the blind birds ($p \leq 0.05$). Most of the time, it was difficult to even distinguish or detect OPs from the blind birds. The amplitudes from the various OPs did not change from one week to another and did not change with increasing stimulus intensity in blind birds. In addition, their implicit times essentially remained consistent. The major difference was seen with the trends of the sighted OPs. In general, with increasing stimulus intensity the amplitudes increased while the implicit times decreased for every OP. Higher amplitudes and faster implicit times was observed for older bird but there was no significant differences ($p \geq 0.05$) compared to other ages. Overall, amplitudes were significantly smaller in blind than sighted for OP1 to OP5 ($p \leq 0.05$) and implicit times were significantly shorter in blind than sighted for OP2 to OP5 ($p \leq 0.05$).

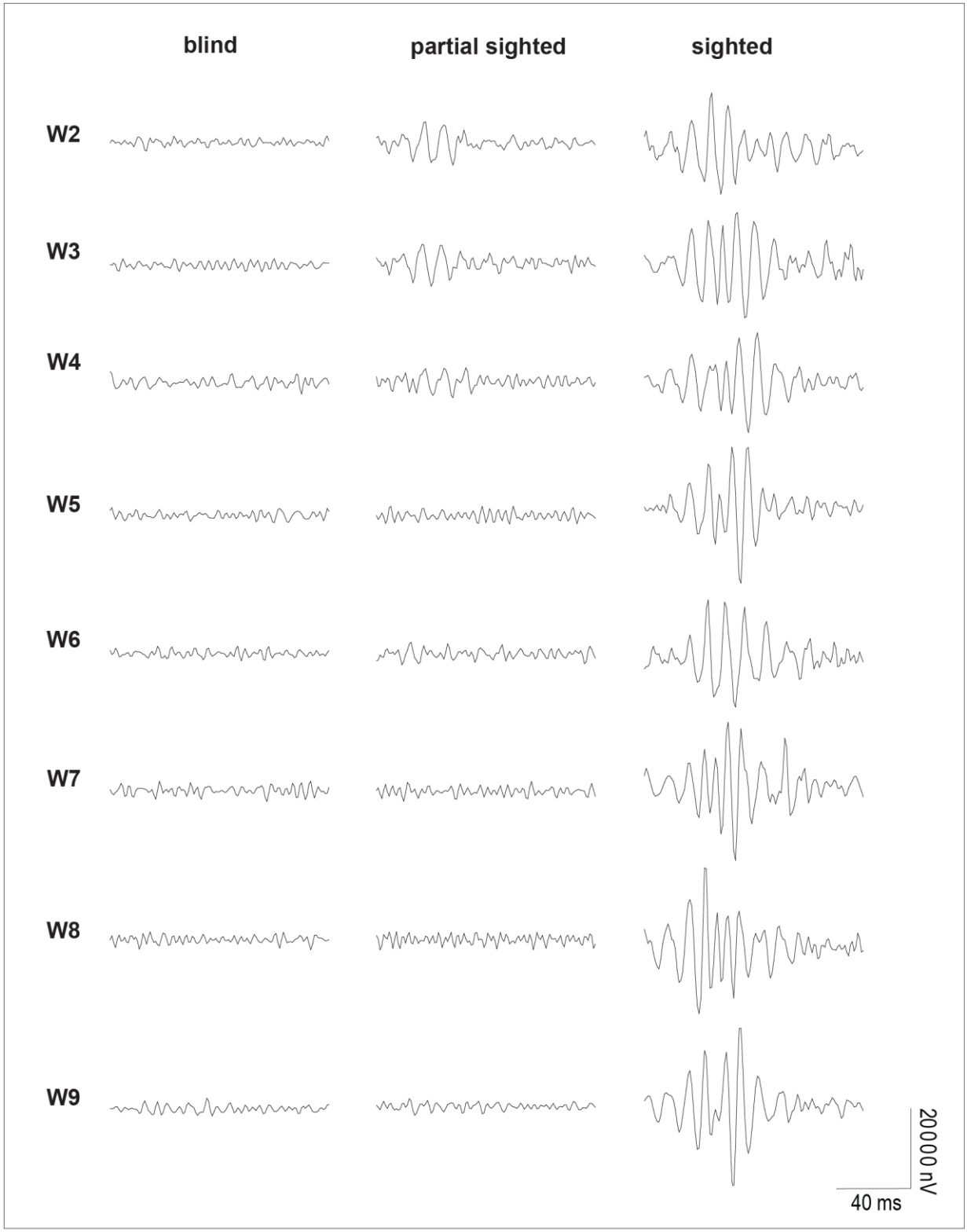

Figure 21. Sample OPs of blind, partial sighted and sigthed SJs across all recorded post-hatch time points.

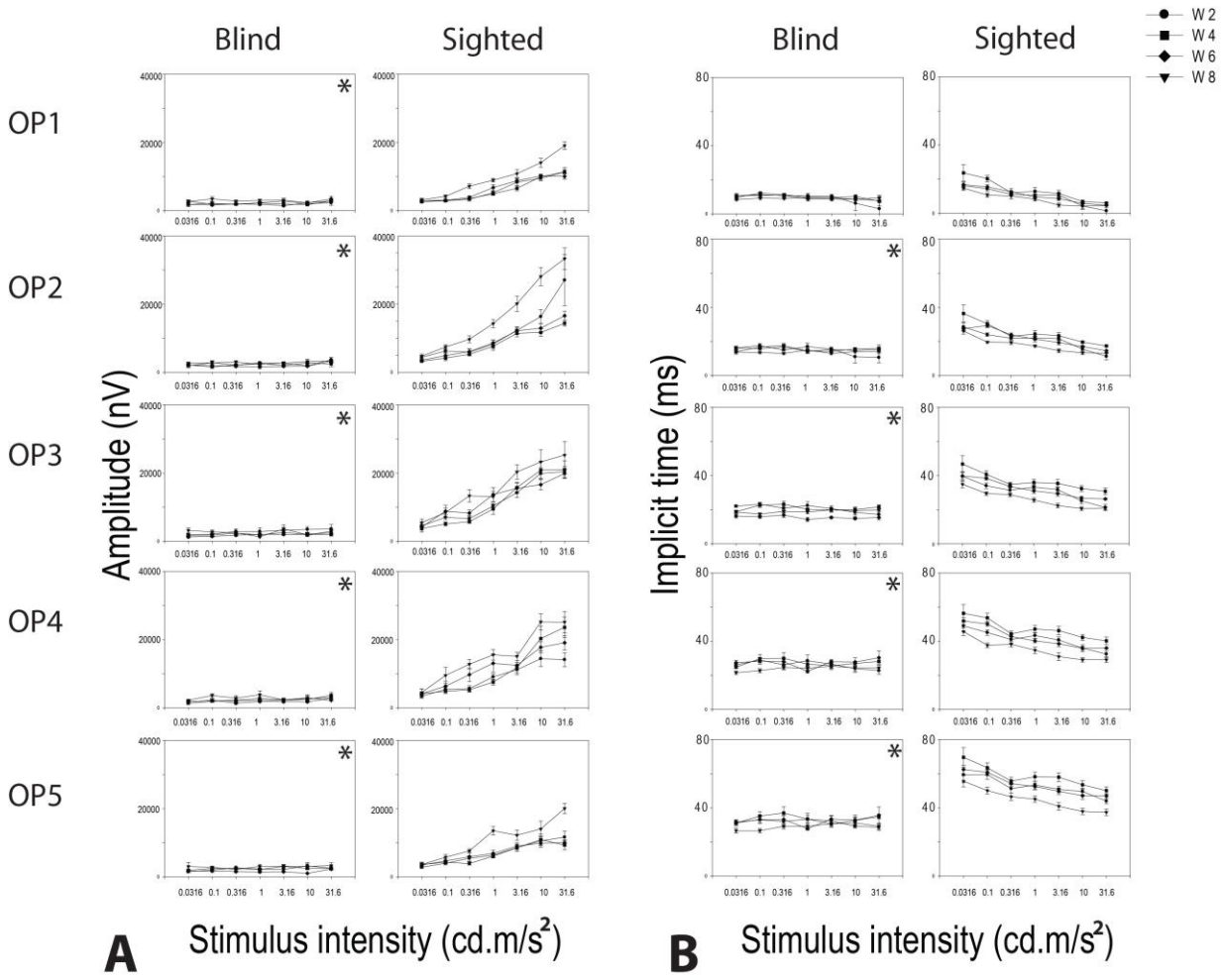

Figure 22. The (A) amplitudes and (B) implicit times of the various OPs at increasing stimulus intensities for time points W2, W4, W6, W8. Asterisks denote significant differences between blind and sighted for each OP over analyzed post-hatch time points.

V. DISCUSSION

5.1 Embryonic development of SJ retinas

Immunofluorescence labeling using cell specific makers allowed developmental observations for each cell type. Visinin is a photoreceptor calcium-binding protein that has been shown to present in developing cones (Hatakenaka et al., 1985; Yamagata et al., 1990), and have been implicated to exist in both rods and cones (Bruhn and Cepko, 1996). During development, cone cells were detected in both blind and sighted birds at E6 which coincides with previous studies (Bruhn and Cepko, 1996). Visinin-positive cell numbers were significantly lower in blind birds throughout development but this was not the case when compared to the percentage of cells, which were similar in both sighted and birds (Figures 7). It is speculated that the difference in visinin-positive cells was only due to the significantly lower total number retinal cells in blind birds. However, in order to state whether a specific cell type is affected, both the number of cells and the percentage of cells must be significantly decreased in blind birds.

For rod cells, a wheat germ agglutinin (WGA) marker was used to bind to the rod cell interphotoreceptor matrix (IPM), a surrounding domain specific to rods (Tien et al., 1992). Embryological rod cells were scarcely detected in the retina of both blind and sighted SJs, appearing in small numbers at E18. Since rod cells in the blind birds were much lower in terms of cell numbers and proportions, these photoreceptors may be a potential target for retinal cell degeneration in SJs in post-hatch birds. The interaction of rods and cones may also be important. Some studies looking at inherited retinal degeneration show that cone cells are affected by neighboring apoptotic rod cells due to release of toxins or viability factors (Bird, 1992; Li et al., 1996).

The expression of Ap2α, a transcription factor, was examined specifically for amacrine

cell differentiation in these SJ chicks. Studies have shown that Ap2α is present exclusively in amacrine cells (Bisgrove and Godbout, 1999; Edqvist and Hallböök, 2004). The delay in amacrine cell development for blind SJs, in which amacrine cells were not detected until E8 versus E6 for sighted embryos, indicate impairment in the differentiation of amacrines from neuroblast cells during embryogenesis. In addition, the overall number of a cells was lower across all time points as their numbers continued to lag behind sighted embryos which further supports the idea of an impairment in amacrine cell development. Since amacrine cells are located within the INL, the lower numbers of cells in the INL of blind birds is attributed to a loss of AP2α amacrines. AP2α is part of a transcription factor family that act as activators (Duan et al., 1995) and repressors (Gaubatz et al., 1995; Getman et al., 1995) of various genes in various tissues. AP2α is shown to suppress the retinal fatty acid binding protein (R-FABP) in chicken (Bisgrove et al., 1997), an analogue of the mammalian brain-FABP, which helps to maintain and establish retinal cell development. FABP studies support the idea of R-FABP being a pivotal inductor of retinal development (Helle et al., 2003). Moreoever, Helle and colleagues, suggest that R-FABP suppression in retinal neurons might suppress growth-inhibitory components that convert normal nerve growth factors into an apoptotic signal. The results of this embryonic experiment lend support to the idea that developmental impairments of AP2α specific amacrine cells in SJs might lead to a similar disinhibition of inhibitory factors that ultimately result in an apoptotic signal and therefore neuronal cell death.

Although no difference was found in the embryonic levels of ganglion, horizontal, bipolar and Müller cells, we cannot exclude a role for their effects on the developmental impairment or degeneration of retinas in the blind embryos. This study examined only the presence or absence of these cells, but no conclusion can be determined about their function(s).

5.2 Retinas in post-hatch SJs

The INL was the observed to be the site of significant cell number reduction in post-hatch blind birds much like the observations in blind embryo retinas of developmental impairment within the INL. The significant loss of cells in the inner portion of the retina further supports the idea that a certain cell type within the INL is affected by the genetic mutation. Interestingly, both the ONL and GCL were observed to have significant differences in total cell numbers between the blind and sighted SJs, although not to such a scale as within the INL. The significant differences in the ONL were not detected until W3, and then again at W6. Detection at a later time point suggests the ONL cells have a later onset of degeneration compared to the cells in the INL. Other mutant chick strains do portray later onset of visual impairment (Randall et al., 1983), and since the severity of blindness is quite varied between SJs, this later effect may account for the delay in SJ blindness for some birds. Similarly, the GCL layers does show a significant difference overall in the total number of cells between blind and sighted but, only show a significance at the last examined time point, W9, which suggest that the GCL does not have a major role in the retinal degeneration for the time points observed. The selected time points were chosen because it was understood that by 8 weeks the blind birds would be completely blind. Unfortunately, the later time points in adult SJs were not examined and potentially could show further effects in the retina.

The total number of retinal cells throughout post-hatch for both blind and sighted birds showed a large decrease at W7 (Figure 11). This large decrease was unexpected for sighted birds. Note that generally, SJs do not become completely blind until W8. Thus, when the birds were collected for enucleation the sighted birds could have been only partially sighted and had yet to develop complete blindness. The retinas from partially blind birds would still

degenerate and lose cells but some vision could remain. Once histologically assessed, these retinas would show loss of cells, observed in Figure 9. It is possible that if these birds were examined at W8, they would have shown complete blindness. Having no assessment of the blind birds genotypes is one of the drawbacks of this study.

In order to follow the development of the putative cone receptor populations, analysis of the numbers and percentages of the visinin-positive cells was maintained for post-hatch chickens despite the idea that visinin is not specific for cones. While most of the evidence for visinin expression in rods were initially observed only in mammalian systems (Polans et al., 1993; Wiechmann and Hammarback, 1993), recent work by Fischer and colleagues (2004) indicates that toxin-induced neurogenic program in post-hatch chick retina can lead to the presence of cells that are labelled for both rhodopsin, a rod-specific marker, and visinin. Therefore, it must be acknowledged that visinin-positive cells in post-hatch chickens are not exclusively cones. Rhodopsin kinase has also been shown to exist in both rods and cones (Zhao et al., 1999). Clearly, rhodopsin kinase labeled cells were more prevalent in the retina than the visinin-positive cells. It remains unclear what cell population the visinin-negative rhodopsin kinase (VnRK)-labeled cells represent.

The finding that the visinin-positive cell numbers and proportions were not different between the blind and sighted birds, suggests that visinin-labeled cells were not the target of degeneration and thus do not contribute to the significant difference of ONL cell between blind and sighted SJs. In constrast, visinin-negative rhodopsin kinase (VnRK)-labeled cells showed significant differences in the number and proportions (Figure 15). These results indicate that VnRK-labeled photoreceptors degenerate within the ONL. Photoreceptor degeneration is a symptom for a number of other inherited hereditary retinal diseases. In chickens, some

characteristics of the SJ birds show similarities to those of the *rd* chicken, in which chicks are not blind at hatch but progressively develop blindness (Ulshafer et al., 1984). Moreover, the *rd* phenotype is characterized by an inability of both photoreceptors to transduce light stimuli due to mutation in the GC1 gene (Semple-Rowland et al., 1996). Although, a mechanism for SJ photoreceptor degeneration cannot be determined from the results it can be speculated that degeneration occurs because of defects in function, much like in other strains.

The findings that amacrine cell numbers and proportions relative to the total cell number are significantly less overall within blind birds compared to sighted birds indicate that amacrines are the initial target of degeneration in the SJs. Even at individual time points, there were significant differences in amacrine cell numbers starting at W3 with progressive decreases up until W9 (Figure 17). The progressive decrease of amacrine cells corresponds with the decrease of cells within the INL. Since the INL is the major contributor to cell number reduction in blind birds, amacrine cells must also have a significant role in SJ retinal degeneration. AP2α has previously been stated to be an important transcription factor during development but if AP2α-amacrine cells continue to degenerate in post-hatch birds, the potential for apoptotic signals to remain active in the mature retina is possible and may cause further degeneration.

In addition to the loss of amacrine cells within the inner retina of the SJ, an effect was seen on the outer layer cells, mainly the photoreceptors. It has been shown that the basic helix-loop-helix (bHLH) chicken gene *cNSCL2*, produced in amacrine and horizontal cells, is involved with retinal development (Li et al., 2001). Although it has been shown that the number of amacrine cells did not decrease due to a misexpression of the *cNSCL2* gene, it did cause effects on photoreceptors and Müller glial cells (Li et al., 2001). Therefore, the results of

this study make it possible to speculate that in the SJ chickens there may be an amacrine cell defect, which not only causes amacrine cell degeneration, but also causes degeneration of photoreceptors. Further studies must therefore focus on using various markers for different amacrine cells in a mature retina based on their biochemical properties for example dopaminergic or cholinergic amacrine cells. Understanding which type of amacrine cell is affected will allow for the determination of future studies.

5.3 ERG analysis of post-hatch birds

ERG analysis of the SJ birds provides further insight in which cells what might be affected within the retina of these birds. Noticeably, initial observations of the ERG recordings showed a greatly diminished response within the blind birds compared to the sighted. The sighted birds actually show similar trends in waveforms, amplitudes and implicit times compared to other recent studies that used wild-type control birds (McGoogan and Cassone, 1999; Montiani-Ferreira et al., 2007). In contrast, the completely blind birds showed affected ERG recordings with no waveforms detected at all (Figure 19). The inability to obtain a recordable ERG suggests that the retinal function in SJ birds is greatly affected by their blindness. Both the a-wave and b-wave were considerably absent in these blind birds. With decreased ERG responses, histologically the SJ retinas showed significant degeneration. This correlates with other findings in which the degeneration of the retina has essentially eliminated the ERG response (Ulshafer et al., 1984). Note the histology revealed significant decreases of VnRK-labeled photoreceptor cells, which were not greatly reduced in blind compared to sighted birds. ERG analysis similarly shows potential functional impairments of both rods and cones. It has also been suggested that a rod-derived cone viability factor exists in some animals, where depletion of rod cells affect the integrity of cone cells (Léveillard et al., 2004). As the rod and

cone populations in this study were not identified, it remains unclear if a similar rod-induced effect on cones existed. Moreover, cones could be affected in older birds at later time points that were not included in this study. Further experiments in which rod and cone function can be measured separately should be done to pinpoint exactly which photoreceptor is affected. For example, the utilization of flicker ERGs would help to distinguish between rods and cones. Note that the birds used for the ERG measurements were not equivalent to the ones used for histology and therefore correlation between the two is not certain.

The single progressively developing blind bird in our batch of chickens allowed a little bit of insight as to what retinal region is affected in terms of ERGs. The ERG recordings of this partially sighted bird showed that there were some measurable a-wave amplitudes as well as very low b-wave amplitudes at an early age (Figure 19). Both a- and b-waves are significantly diminished in amplitude with the b-wave amplitudes being affected earlier compared to sighted birds. This suggests that cells of the inner retina from the b-wave, amacrines and bipolars, are affected functionally before the photoreceptor cells, and derived from the a-wave, which is consistent with histological evidence. The shape of the ERG waveform from this partially sighted bird is also similar to that of other mutant chicks such as *rge* and DAMS strains. They show similar decreases in a-wave amplitudes and longer implicit times in addition to greatly reduced b-wave amplitudes (Fulton et al., 1983; Montiani-Ferreira et al., 2007). At W5-W6 time points, the ERGs of this partially sighted bird were completely eliminated in conjunction with the complete blindness at around this same time point. The abolishment of ERG responses due to complete blindness and the progressive nature of the one partially sighted bird highlight the need for future experiments, to obtain SJs that start off with sight but will later become blind. In addition the genetic component of these birds needs to be

assessed as an essential part of further understanding.

The diminished OP amplitudes measured for the blind birds were expected as b-waves were barely detectable. Similar to the ERGs, OP responses were hardly detected for the blind birds compared to those of the sighted birds. The partially sighted bird showed some very low OP wavelets with small amplitudes (Figure 21). By W3-W4 these OPs disappeared and were not detected again. Analysis of the various OPs within the blind chicks revealed that their amplitudes did not change with intensity and maintained really low amplitudes, essentially indicating an absence of a response. In contrast, sighted birds with presumably functioning retinal cells showed that with increasing stimulus the measured amplitudes increased and implicit times decreased for OPs. This general trend has been documented in previous OP studies (Liu et al., 2006). Therefore the trends seen in the sighted birds and not seen in the blind suggest that inner retinal cell function is non-existent in these blind chicks. The fact that the b-wave and OPs are affected first (followed by a-wave depletion) correlates with the histological observations that the INL is targeted first for degeneration in the blind SJs.

In summary, the results of this study indicate that the SJ blind birds start off with lower amounts of cells within their retina due to impairments of development. Following hatch, some birds are already blind while others develop the blindness with age. The developing blindness coincides with the progressive nature of degeneration that occurs in the retina post-hatch. The changes were mainly detected within the inner layer of the retina (INL) throughout both embryonic development and post-hatch chicks. Consequently, amacrine cells, which reside in the INL, were the significant cell type to contribute to the retinal degeneration. In addition, VnRK-labelled photoreceptors were identified as secondary contributors to the decrease of cell numbers as they were seen to affect post-hatch blind birds. Presumably, loss

of rod function, represented by the abolishment of ERG a-waves, reflects that rods are the specific cell type affected in the VnRK-labeled cell population. The effects of the amacrine were further confirmed with ERG measurements showing an abolishment of the OPs/b-waves. Note that the blindness in SJs did not allow for many recordable ERGs to be detected. Now that potential cell types have been identified as the cause of degeneration in the SJ chicks, future studies must focus on more detailed aspects of the cells. In particular, which types of amacrine cells are affected, in addition to the mechanism by which the cells are degenerating, are of interest. In addition, as mentioned above, the studies on the progressive blindness in these chicks might help in identifying particular aspects of the ERG that are affected before the response is completely eliminated. Collaborations are in progress to determine genetic information of the SJ mutant strain. That way studies can then be pinpointed towards specific pathways of interest.

REFERENCES

Araki, M., Fukada, Y., Shichida, Y. and Yoshizawa, T. (1990). Localization of iodopsin in the chick retina during in vivo and in vitro cone differentiation. *Investigative Ophthalmology & Visual Science* **31**, 1466–1473.

Asi, H. and Perlman, I. D. O. (1992). Relationships between the electroretinogram a-wave , b-wave and oscillatory potentials and their application to clinical diagnosis The electroretinogram (ERG) is a complex electrical signal that is recorded. *Documenta Ophthalmologica* 1992–1992.

Beaudet, A., Cuénod, M. and Reubi, J. C. (1981). Selective bidirectional transport of [3H]d-aspartate in the pigeon retino-tectal pathway. *Neuroscience* **6**, 2021–2034.

Bird, A. C. (1992). Investigation of disease mechanisms in retinitis pigmentosa. *Ophthalmic Paediatrics And Genetics* **13**, 57–66.

Bisgrove, D. A. and Godbout, R. (1999). Differential expression of AP-2alpha and AP-2beta in the developing chick retina: repression of R-FABP promoter activity by AP-2. *Developmental dynamics an official publication of the American Association of Anatomists* **214**, 195–206.

Bisgrove, D. A., Monckton, E. A. and Godbout, R. (1997). Involvement of AP-2 in regulation of the R-FABP gene in the developing chick retina. *Molecular and Cellular Biology* **17**, 5935–5945.

Biziere, K. and Coyle, J. T. (1979). Localization of receptors for kainic acid on neurons in the innernuclear layer of retina. *Neuropharmacology* **18**, 409–413.

Bovolenta, P., Mallamaci, A., Briata, P., Corte, G. and Boncinelli, E. (1997). Implication of OTX2 in pigment epithelium determination and neural retina differentiation. *Journal of Neuroscience* **17**, 4243–4252.

Britto, L. R. G., Keyser, K. T., Hamassaki, D. E. and Karten, H. J. (1988). Catecholaminergic subpopulation of retinal displaced ganglion cells projects to the accessory optic nucleus in the pigeon (Columba livia). *The Journal of Comparative Neurology* **269**, 109–117.

Brown, K. T. and Watanabe, K. (1962). Isolation and identification of a receptor potential from the pure cone fovea of the monkey retina. *Nature* **193**, 958 passim.

Brown, K. T. and Wiesel, T. N. (1961). Localization of origins of electroretinogram components by intraretinal recording in the intact cat eye. *The Journal of Physiology* **158**, 257–280.

Bruhn, S. L. and Cepko, C. L. (1996). Development of the pattern of photoreceptors in the chick retina. *Journal of Neuroscience* **16**, 1430–1439.

Cheng, K. M., Shoffner, R. N., Gelatt, K. N., Gum, G. G., Otis, J. S. and Bitgood, J. J. (1980). An autosomal recessive blind mutant in the chicken. *Poultry Science* 59, 2179–2181.

Coulombre, J. L. and Coulombre, A. J. (1965). Regeneration of neural retina from the pigmented epithelium in the chick embryo. *Developmental Biology* **12**, 79–92.

Curtis, P. E., Baker, J. R., Curtis, R. and Johnston, A. (1987). Impaired vision in chickens associated with retinal defects. *Veterinary Record* **120**, 113–114.

Den Hollander, A. I., Roepman, R., Koenekoop, R. K. and Cremers, F. P. M. (2008). Leber congenital amaurosis: genes, proteins and disease mechanisms. *Progress in Retinal and Eye Research* **27**, 391–419.

Dong, C. J. and Hare, W. A. (2000). Contribution to the kinetics and amplitude of the electroretinogram b-wave by third-order retinal neurons in the rabbit retina. *Vision Research* **40**, 579–589.

Duan, C., Clemmons, D. R., Hill, C. and Carolina, N. (1995). Transcription Factor AP-2 Regulates Human Insulin-like Growth Factor Binding Protein-5 Gene Expression. *J Biol Chem* **270**, 24844 –24851.

Edqvist, P.-H. D. and Hallböök, F. (2004). Newborn horizontal cells migrate bi-directionally across the neuroepithelium during retinal development. *Development* **131**, 1343–51.

Ehrlich, D. (1981). Regional specialization of the chick retina as revealed by the size and density of neurons in the ganglion cell layer. *Journal of Comparative Neurology* **195**, 643–657.

Einthoven, W. and Jolly, W. A. (1908). The form and magnitude of the electrical response of the eye to stimulation by light at various intensities. *Experimental Physiology* **1**, 373–416.

Fischer, A. J., Wang, S.-Z. and Reh, T. A. (2004). NeuroD induces the expression of visinin and calretinin by proliferating cells derived from toxin-damaged chicken retina. *Developmental dynamics an official publication of the American Association of Anatomists* **229**, 555–563.

Fite, K. V., Montgomery, N., Whitney, T., Boissy, R. and Smyth, J. R. (1982). Inherited retinal degeneration and ocular amelanosis in the domestic chicken (Gallus domesticus). *Current Eye Research* **2**, 109–115.

Franceschetti, A. and Dieterle, P. (1954). Diagnostic and prognostic importance of the electroretinogram in tapetoretinal degeneration with reduction of the visual field and hemeralopia. *Confinia Neurologica* **14**, 184–186.

Fulton, A. B., Fite, K. V. and Bengston, L. (1983). Retinal degeneration in the delayed amelanotic (DAM) chicken: an electro- retinographic study. *Current eye research* **2**, 757–763.

Gaubatz, S., Imhof, A., Dosch, R., Werner, O., Mitchell, P., Buettner, R. and Eilers, M. (1995). Transcriptional activation by Myc is under negative control by the transcription factor AP-2. *the The European Molecular Biology Organization Journal* **14**, 1508–1519.

Getman, D. K., Mutero, A., Inoue, K. and Taylor, P. (1995). Transcription factor repression and activation of the human acetylcholinesterase gene. *The Journal of Biological Chemistry* **270**, 23511–23519.

Goto, Y., Yasuda, T., Tobimatsu, S. and Kato, M. (1998). 20-Hz flicker stimulus can isolate the cone function in rat retina. *Ophthalmic Research* **30**, 368–373.

Granit, R. (1933). The components of the retinal action potential in mammals and their relation to the discharge in the optic nerve. *The Journal of Physiology* **77**, 207–239.

Hageman, G. S., Luthert, P. J., Victor Chong, N. H., Johnson, L. V., Anderson, D. H. and Mullins, R. F. (2001). An integrated hypothesis that considers drusen as biomarkers of immune-mediated processes at the RPE-Bruch's membrane interface in aging and age-related macular degeneration. *Progress in Retinal and Eye Research* **20**, 705–732.

Hamel, C. (2001). Retinitis pigmentosa. *Orphanet Journal of Rare Diseases* **20**, 40.

Hanawa, I., Takahashi, K. and Kawamoto, N. (1976). A correlation of embryogenesis of visual cells and early receptor potential in the developing retina. *Experimental Eye Research* **23**, 587–594.

Hatakenaka, S., Kiyama, H., Tohyama, M. and Miki, N. (1985). Immunohistochemical localization of chick retinal 24 kdalton protein (visinin) in various vertebrate retinae. *Brain Research* **331**, 209–215.

Helle, T., Deiss, S., Schwarz, U. and Schlosshauer, B. (2003). Glial and neuronal regulation of the lipid carrier R-FABP. *Experimental Cell Research* **287**, 88–97.

Heynen, H., Wachtmeister, L. and Van Norren, D. (1985). Origin of the oscillatory potentials in the primate retina. *Vision Research* **25**, 1365–1373.

Hood, D. C., Seiple, W., Holopigian, K. and Greenstein, V. (1997). A comparison of the components of the multifocal and full-field ERGs. *Visual Neuroscience* **14**, 533–544.

Hughes, W. F. and McLoon, S. C. (1979). Ganglion cell death during normal retinal development in the chick: comparisons with cell death induced by early target field destruction. *Experimental Neurology* **66**, 587–601.

Hyer, J., Mima, T. and Mikawa, T. (1998). FGF1 patterns the optic vesicle by directing the placement of the neural retina domain. *Development* **125**, 869–877.

Ikeda, A., Yoshii, I. and Mishima, N. (1980). An immunohistochemical study of the Müller cells of the chicken retina. *Archivum histologicum Japonicum Nippon soshikigaku kiroku* **43**, 175–183.

Inglehearn, C. F., Morrice, D. R., Lester, D. H., Robertson, G. W., Mohamed, M. D., Simmons, I., Downey, L. M., Thaung, C., Bridges, L. R., Paton, I. R., et al. (2003). Genetic, ophthalmic, morphometric and histopathological analysis of the Retinopathy Globe Enlarged

(rge) chicken. *Molecular Vision* 9, 295–300.

Kirkham, T. H. and Coupland, S. G. (1983). The pattern electroretinogram in optic nerve demyelination. *The Canadian journal of neurological sciences Le journal canadien des sciences neurologiques* **10**, 256–260.

Koenekoop, R. K. (2004). An overview of Leber congenital amaurosis: a model to understand human retinal development. *Survey of Ophthalmology* **49**, 379–398.

Kolb, H. and Gouras, P. (1974). Electron microscopic observations of human retinitis pigmentosa, dominantly inherited. *Investigative Ophthalmology* **13**, 487–498.

Korol, S., Leuenberger, P. M., Englert, U. and Babel, J. (1975). In vivo effects of glycine on retinal ultrastructure and averaged electroretinogram. *Brain Research* **97**, 235–251.

Kuszak, J., Alcala, J. and Maisel, H. (1980). The surface morphology of embryonic and adult chick lens-fiber cells. *The American journal of anatomy* **159**, 395–410.

Lai, T. Y. Y., Chan, W.-M., Lai, R. Y. K., Ngai, J. W. S., Li, H. and Lam, D. S. C. (2007). The clinical applications of multifocal electroretinography: a systematic review. *Survey of Ophthalmology* **52**, 61–96.

Lei, B. and Perlman, I. (1999). The contributions of voltage- and time-dependent potassium conductances to the electroretinogram in rabbits. *Visual Neuroscience* **16**, 743–754.

Li, T., Snyder, W. K., Olsson, J. E. and Dryja, T. P. (1996). Transgenic mice carrying the dominant rhodopsin mutation P347S: evidence for defective vectorial transport of rhodopsin to the outer segments. *Proceedings of the National Academy of Sciences of the United States of America* **93**, 14176–14181.

Li, C. M., Yan, R. T. and Wang, S. Z. (2001). Atrophy of Müller glia and photoreceptor cells in chick retina misexpressing cNSCL2. *Investigative Ophthalmology & Visual Science* **42**, 3103–3109.

Liu, K., Akula, J. D., Hansen, R. M., Moskowitz, A., Kleinman, M. S. and Fulton, A. B. (2006). Development of the electroretinographic oscillatory potentials in normal and ROP rats. *Investigative Ophthalmology & Visual Science* **47**, 5447–5452.

Léveillard, T., Mohand-Saïd, S., Lorentz, O., Hicks, D., Fintz, A.-C., Clérin, E., Simonutti, M., Forster, V., Cavusoglu, N., Chalmel, F., et al. (2004). Identification and characterization of rod-derived cone viability factor. *Nature Genetics* 36, 755–759.

Mafei, L. and Fiorentini, A. (1981). Electroretinographic responses to alternating gratings before and after section of the optic nerve. *Science* **211**, 953–955.

Maffei, L., Fiorentini, A., Bisti, S. and Holländer, H. (1985). Pattern ERG in the monkey after section of the optic nerve. *Experimental Brain Research* **59**, 423–425.

Marmor, M. F., Holder, G. E., Seeliger, M. W. and Yamamoto, S. (2004). Standard for clinical electroretinogram. *Documenta Ophthalmologica* **108**, 107–114.

McGoogan, J. M. and Cassone, V. M. (1999). Circadian regulation of chick electroretinogram: effects of pinealectomy and exogenous melatonin. *American Journal of Physiology* **277**, R1418–R1427.

Mey, J. and Thanos, S. (2000). Development of the visual system of the chick. I. Cell differentiation and histogenesis. *Brain research Brain research reviews* **32**, 343–379.

Mizuno, K. and Nishida, S. (1967). Electron microscopic studies of human retinitis pigmentosa. I. Two cases of advanced retinitis pigmentosa. *American Journal of Ophthalmology* **63**, 791–803.

Mochii, M., Mazaki, Y., Mizuno, N., Hayashi, H. and Eguchi, G. (2011). Role of Mitf in differentiation and transdifferentiation of chicken pigmented epithelial cell. *Optics Express* **19**, 47–62.

Montiani-Ferreira, F., Li, T., Kiupel, M., Howland, H., Hocking, P., Curtis, R. and Petersen-Jones, S. (2003). Clinical features of the retinopathy, globe enlarged (rge) chick phenotype. *Vision Research* **43**, 2009–2018.

Montiani-Ferreira, F., Shaw, G. C., Geller, A. M. and Petersen-Jones, S. M. (2007). Electroretinographic features of the retinopathy, globe enlarged (rge) chick phenotype. *Molecular Vision* **13**, 553–565.

Murakami, M. and Kaneko, A. (1966). Sub components of P3 in cold-blooded vertebrate retinae. *Nature* **210**, 103–104.

Nishimura, Y. (1980). Determination of the developmental pattern of retinal ganglion cells in chick embryos by Golgi impregnation and other methods. *Anatomy and Embryology* **158**, 329–347.

Ogden, T. E. (1973). The oscillatory waves of the primate electroretinogram. *The Journal of general physiology* **46**, 1059–1074.

Okano, T., Kojima, D., Fukada, Y., Shichida, Y. and Yoshizawa, T. (1992). Primary structures of chicken cone visual pigments: vertebrate rhodopsins have evolved out of cone visual pigments. *Proceedings of the National Academy of Sciences of the United States of America* **89**, 5932–5936.

Olson, M. D. (1979). Scanning electron microscopy of developing photoreceptors in the chick retina. *The Anatomical record* **193**, 423–438.

O'Rahilly, R. and Meyer, D. B. (1959). The early development of the eye in the chick. Gallus Domesticus (stages 8 to 25). *Acta Anatomica* 20–58.

Park, C. M. and Hollenberg, M. J. (1989). Basic fibroblast growth factor induces retinal

regeneration in vivo. *Developmental Biology* **134**, 201–205.

Pepperberg, D. R. and Masland, R. H. (1978). Retinal-induced sensitization of light-adapted rabbit photoreceptors. *Brain Research* **151**, 194–200.

Pepperberg, D. R., Brown, P. K., Lurie, M. and Dowling, J. E. (1978). Visual pigment and photoreceptor sensitivity in the isolated skate retina. *The Journal of general physiology* **71**, 369–396.

Pittack, C., Grunwald, G. B. and Reh, T. A. (1997). Fibroblast growth factors are necessary for neural retina but not pigmented epithelium differentiation in chick embryos. *Development Cambridge England* **124**, 805–816.

Polans, A. S., Burton, M. D., Haley, T. L., Crabb, J. W. and Palczewski, K. (1993). Recoverin, but not visinin, is an autoantigen in the human retina identified with a cancer-associated retinopathy. *Investigative Ophthalmology & Visual Science* **34**, 81–90.

Pollock, B. J., Wilson, M. A. and Randall, C. J. (1982). Preliminary observations of a new blind chick mutant (beg). In *Problems of Normal and Genetically Abnormal Retinas* (ed. Clayton, R. M., Haywood, J., Reading, H. W., and Right, A. W.), pp. 241–248. London: Academic Press.

Prada, C., Puelles, L. and Génis-Gálvez, J. M. (1981). A golgi study on the early sequence of differentiation of ganglion cells in the chick embryo retina. *Anatomy and Embryology* **161**, 305–317.

Prada, F. A., Quesada, A., Dorado, M. E., Chmielewski, C. and Prada, C. (1998). Glutamine synthetase (GS) activity and spatial and temporal patterns of GS expression in the developing chick retina: relationship with synaptogenesis in the outer plexiform layer. *Glia* **22**, 221–236.

Quesada, A., Garcia-Lomas, V. and Genis-Galvez, J. M. (1986). The midget bipolar cells in the chick retina. *Current Eye Research* **5**, 85–92.

Randall, C. J., Wilson, M. A., Pollock, B. J., Clayton, R. M., Ross, A. S., Bard, J. B. and McLachlan, I. (1983). Partial retinal dysplasia and subsequent degeneration in a mutant strain of domestic fowl (rdd). *Experimental Eye Research* **37**, 337–347.

Salter, D. W., Payne, W. S., Ramsey, D. T., Blair, M. and Render, J. A. (1997). A new inherited ocular anomaly in pigmented white Leghorn chickens. *Journal of Veterinary Diagnostic Investigation* **9**, 407–409.

Sellheyer, K. (1990). Development of the choroid and related structures. *Eye London England* **4 (Pt 2)**, 255–261.

Semple-Rowland, S. L., Gorczyca, W. A., Buczylko, J., Helekar, B. S., Ruiz, C. C., Subbaraya, I., Palczewski, K. and Baehr, W. (1996). Expression of GCAP1 and GCAP2 in the retinal degeneration (rd) mutant chicken retina. *FEBS Letters* 385, 47–52.

Semple-Rowland, S. L., Lee, N. R., Van Hooser, J. P., Palczewski, K. and Baehr, W. (1998). A null mutation in the photoreceptor guanylate cyclase gene causes the retinal degeneration chicken phenotype. *Proceedings of the National Academy of Sciences of the United States of America* **95**, 1271–1276.

Sieving, P. A., Frishman, L. J. and Steinberg, R. H. (1986). Scotopic threshold response of proximal retina in cat. *Journal of Neurophysiology* **56**, 1049–1061.

Sillman, A. J., Ito, H. and Tomita, T. (1969). Studies on the mass receptor potential of the isolated frog retina. I. General properties of the response. *Vision Research* **9**, 1435–1442.

Smyth, J. R., Boissy, R. E. and Fite, K. V. (1981). The DAM chicken: a model for spontaneous postnatal cutaneous and ocular amelanosis. *The Journal of Heredity* **72**, 150–156.

Snell, R. S. and Lemp, M. A. (1989). *Clinical Anatomy of the Eye*. 1st ed. (ed. Snell, R. S. and Lemp, M. A.) Boston: Blackwell Scientific.

Spira, A. W., Millar, T. J., Ishimoto, I., Epstein, M. L., Johnson, C. D., Dahl, J. L. and Morgan, I. G. (1987). Localization of choline acetyltransferase-like immunoreactivity in the embryonic chick retina. *Journal of Comparative Neurology* **260**, 526–538.

Steinberg, R. H. (1966). Oscillatory activity in the optic tract of cat and light adaptation. *Journal of Neurophysiology* **29**, 139–156.

Straznicky, C. and Chehade, M. (1987). The formation of the area centralis of the retinal ganglion cell layer in the chick. *Development Cambridge England* **100**, 411–420.

Szamier, R. B., Berson, E. L., Klein, R. and Meyers, S. (1979). Sex-linked retinitis pigmentosa: ultrastructure of photoreceptors and pigment epithelium. *Investigative Ophthalmology & Visual Science* **18**, 145–160.

Thanos, S., Vanselow, J. and Mey, J. (1992). Ganglion cells in the juvenile chick retina and their ability to regenerate axons in vitro. *Experimental Eye Research* **54**, 377–391.

Tien, L., Rayborn, M. E. and Hollyfield, J. G. (1992). Characterization of the interphotoreceptor matrix surrounding rod photoreceptors in the human retina. *Experimental Eye Research* **55**, 297–306.

Tomita, T. (1950). Studies on the intraretinal action potential. I. Relation between the localization of micropipette in the retina and the shape of the intraretinal action potential. *Japanese Journal of Physiology* **1**, 110–117.

Trick, G. L. and Wintermeyer, D. H. (1982). Spatial and temporal frequency tuning of pattern-reversal retinal potentials. *Investigative Ophthalmology & Visual Science* **23**, 774–779.

Tummala, H., Ali, M., Getty, P., Hocking, P. M., Burt, D. W., Inglehearn, C. F. and Lester, D. H. (2006). Mutation in the guanine nucleotide-binding protein beta-3 causes retinal degeneration and embryonic mortality in chickens. *Investigative Ophthalmology & Visual*

Science **47**, 4714–4718.

Ulshafer, R. J., Allen, C., Dawson, W. W. and Wolf, E. D. (1984). Hereditary retinal degeneration in the Rhode Island Red chicken. I. Histology and ERG. *Experimental Eye Research* **39**, 125–135.

Vanselow, J., Dütting, D. and Thanos, S. (1990). Target dependence of chick retinal ganglion cells during embryogenesis: cell survival and dendritic development. *Journal of Comparative Neurology* **295**, 235–247.

Vorobyev, M. (2003). Coloured oil droplets enhance colour discrimination. *Proceedings of the Royal Society B Biological Sciences* **270**, 1255–1261.

Wachtmeister, L. and Dowling, J. E. (1978). The oscillatory potentials of the mudpuppy retina. *Investigative Ophthalmology & Visual Science* **17**, 1176–1188.

Warwick, R. and Williams, P. L. (1973). *Gray's Anatomy 35th British ed.* 35th ed. (ed. Saunders, W. B.) Philadelphia: Longman.

Watanabe, M., Rutishauser, U. and Silver, J. (1991). Formation of the retinal ganglion cell and optic fiber layers. *Journal of Neurobiology* **22**, 85–96.

Wiechmann, A. F. and Hammarback, J. A. (1993). Expression of recoverin mRNA in the human retina: localization by in situ hybridization. *Experimental Eye Research* **57**, 763–769.

Willbold, E. and Layer, P. G. (1992). Formation of neuroblastic layers in chicken retinospheroids: the fibre layer of Chievitz secludes AChE-positive cells from mitotic cells. *Cell and Tissue Research* **268**, 401–408.

Winkler, B. S., Kapousta-Bruneau, N., Arnold, M. J. and Green, D. G. (1999). Effects of inhibiting glutamine synthetase and blocking glutamate uptake on b-wave generation in the isolated rat retina. *Visual Neuroscience* **16**, 345–353.

Witkovsky, P., Dudek, F. E. and Ripps, H. (1975). Slow PIII component of the carp electroretinogram. *The Journal of general physiology* **65**, 119–134.

Wulle, I. and Wagner, H. J. (1990). GABA and tyrosine hydroxylase immunocytochemistry reveal different patterns of colocalization in retinal neurons of various vertebrates. *Journal of Comparative Neurology* **296**, 173–178.

Yamagata, M. and Sanes, J. R. (1995). Target-independent diversification and target-specific projection of chemically defined retinal ganglion cell subsets. *Development Cambridge England* **121**, 3763–3776.

Yamagata, K., Goto, K., Kuo, C. H., Kondo, H. and Miki, N. (1990). Visinin: a novel calcium binding protein expressed in retinal cone cells. *Neuron* **4**, 469–476.

Zhao, X., Yokoyama, K., Whitten, M. E., Huang, J., Gelb, M. H. and Palczewski, K.

(1999). A novel form of rhodopsin kinase from chicken retina and pineal gland. *FEBS Letters* **454**, 115–121.